A model reduction strategy for computing the forced response of elastic waveguides using the wave finite element method

Jean-Mathieu Mencik

A model reduction strategy for computing the forced response of elastic waveguides using the wave finite element method

J.-M. Mencik

ENI Val de Loire, Université François Rabelais de Tours, LMR laboratory, Rue de la Chocolaterie, BP 3410, F-41034 Blois Cedex, France

Abstract

A model reduction strategy is proposed within the framework of the wave finite element method for computing the low- and mid-frequency forced response of single and coupled straight elastic waveguides. For any waveguide, a norm-wise error analysis is proposed for efficiently reducing the size of the wave basis involved in the description of the dynamic behavior. The strategy is validated through the following test cases: single and coupled beam-like structures with thick cross-sections, plates and sandwich structures. The relevance of the model reduction strategy for saving large CPU times is highlighted, considering the computation of the acoustic radiation of plates and Monte Carlo simulations of coupled waveguides.

Key words: Wave finite elements, model reduction, mid-frequencies, acoustic radiation.

1. Introduction

This paper addresses, within the framework of the wave finite element (WFE), a model reduction strategy of matrix formulations for computing the low- and mid-frequency (LF and MF) forced response of single and coupled straight elastic

waveguides. Some of these elastic systems are depicted in Figure 1 (i.e. single and coupled beam-like structures with thick cross-sections, plates and sandwich structures). Within the MF framework, the cross-sections of waveguides are expected to undergo oscillating spatial dynamics as well as local resonances. The WFE method aims at computing the LF and MF wave modes which travel along any waveguide in positive and negative directions. The computation of the wave modes results from a finite element (FE) procedure which enables the waveguide cross-section to be discretized by means of several degrees of freedom (DOFs). The number of wave modes is actually linked to that of the DOFs used for discretizing the cross-section, which implicitly depends on the excitation frequency. For example, a large number of wave modes can be required to capture the MF behavior, i.e. when the cross-section undergoes oscillating dynamics. WFE matrix formulations have been deeply investigated in a former paper [1] for computing the harmonic responses of waveguides such as those depicted in Figure 1 (other works can be found in [2, 3]). These formulations use reduced bases of wave modes to capture the waveguide dynamics in the LF and MF range. Reducing these wave bases efficiently, in terms of wave modes which effectively contribute for expressing the waveguide behavior, appears crucial in many applications (e.g. acoustic radiation of plates where a large number of coupling terms need to be computed at many frequency steps, or Monte Carlo simulations (MCS) involving a large number of iterations).

The strategy for selecting the contributing wave modes constitutes the motivation behind the present paper. The issue is to provide an alternative solution to the commonly used strategy that consists in retaining the wave modes which are propagating at a certain frequency [1]. The drawback of such a selection procedure is that the wave modes are ranked in accordance to the imaginary parts of their wavenumbers, regardless of their contribution to the structure behavior. In fact, should a few high order modes (i.e. whose wavenumbers exhibit high imaginary

parts) contribute to the forced response, the classic procedure states that almost the full wave basis has to be considered. Proposing another strategy for efficiently selecting the contributing wave modes constitutes an open challenge. The final goal is to propose wave bases with optimal reduced sizes with a view to reducing CPU times for computing the forced responses of waveguides.

Model order reduction (MOR) techniques have been widely treated in the literature within the frameworks of CMS approaches [4], SVD-based and Krylov-based methods [5]. Within the CMS framework, an optimal modal reduction technique based on the study of an error norm for coupling interface forces has been proposed in refs. [6, 7]. A moment matching method (i.e. which considers low order terms of Taylor series around some pulsation ω) that investigates displacement vectors over coupling interfaces has been proposed in ref. [8]. Moment matching approaches have also been addressed from the point of view of Krylov subspace techniques for estimating scalar transfer functions with minimum error [9]. Finally, a Rational Krylov based model reduction method that investigates matrix-valued transfer functions of single-input multi-output (SIMO) dynamic systems has been proposed in refs. [10, 11]. Other discussions on SVD-based methods can be found in refs. [5, 12].

Although the aforementioned MOR techniques seem interesting yet, their application to WFE matrix formulations does not seem straightforward. The first difficulty is that WFE-based transfer functions are more complicated than those involved by other MOR techniques; the issue is that most of the matrices involved by the WFE formulations depend on the frequency, as opposed to classic FE approaches where conventional mass / stiffness matrices are rather of concern. The second difficulty lies in the fact that wave bases are not orthogonal, which means that matrix systems cannot be decoupled into sets of independent equations. The problem turns out to be as follows: among all the wave modes $\{\mathbf{\Phi}_j\}_{j=1,\ldots,2n}$

whose amplitudes are $\{Q_j\}_j$, extract a reduced family $\{\widetilde{\boldsymbol{\Phi}}_j\}_{j=1,\ldots,2m}$ $(m \leq n)$ with amplitudes $\{\widetilde{Q}_j\}_j$ such that $\widetilde{Q}_j \approx Q_j \; \forall j \in \{1,\ldots,2m\}$ and $Q_j \approx 0$ $\forall j \in \{2m+1,\ldots,2n\}$, taking into account that the wave modes $\{\boldsymbol{\Phi}_j\}_j$ are not orthogonal. In matrix form, this yields the following error norms $||\widetilde{\mathbf{Q}} - \widetilde{\mathcal{L}}\mathbf{Q}||$ and $||\mathcal{L}_{\mathbf{r}}\mathbf{Q}||$ to be assessed and minimized, where $\widetilde{\mathcal{L}}$ and $\mathcal{L}_{\mathbf{r}}$ play the role of incidence matrices. Reducing these error norms by means of a basis of wave modes $\{\widetilde{\boldsymbol{\Phi}}_j\}_j$ with optimal reduced size constitutes an original challenge which is addressed within the present study.

The key idea behind the proposed MOR procedure is to invoke a finite number of forward / backward passings of waves along any waveguide for expressing the wave amplitudes $\{\widetilde{Q}_j\}_j$. In this framework, it is shown that the error induced for expressing the waveguide displacements and forces can be bounded in terms of matrix norms which are not necessarily decreasing functions of the number of retained wave modes. The resulting error bound is found to be sensitive – that is, it increases – when the size of the wave basis is overestimated. Thus, the problem is to find a minimum for such an error bound with regard to the number of retained wave modes. This constitutes an efficient strategy to determine precisely the number of wave modes required to compute the forced response of waveguides accurately.

The rest of the paper is organized as follows. The WFE framework is recalled in Section 2; also, the concept of model reduction involving the error norms $||\widetilde{\mathbf{Q}} - \widetilde{\mathcal{L}}\mathbf{Q}||$ and $||\mathcal{L}_{\mathbf{r}}\mathbf{Q}||$ (see above) is presented. The MOR strategy is detailed in Section 3, considering the single waveguide case; bounds of the aforementioned error norms are detailed; the procedure that invokes a finite number of forward / backward passings of waves along waveguides, for expressing the wave amplitudes, is detailed; an error bound of $||\widetilde{\mathbf{Q}} - \widetilde{\mathcal{L}}\mathbf{Q}|| + ||\mathcal{L}_{\mathbf{r}}\mathbf{Q}||$ is proposed; it is shown that the minimization of this error bound yields the wave modes which effectively

4

contribute to the waveguide behavior to be selected efficiently. The case of coupled systems involving two waveguides connected through an elastic junction is fully investigated in Section 4. Numerical experiments are brought in Section 5; the frequency forced responses of single and coupled waveguides are simulated; the accuracy of the MOR strategy for describing the waveguide forced responses with a few wave modes is highlighted; also, the efficiency of the MOR strategy for saving large CPU times is highlighted, considering the computation of the acoustic radiation of a square plate as well as Monte Carlo simulations involving two waveguides connected with an elastic junction (whose eigenfrequencies are uncertain).

2. WFE method

2.1. Theory

The WFE method has been originally developed for describing numerically the waves traveling along periodic structures [13]. Such structures are called periodic in the sense that they can be described by means of similar substructures, with the same length d, which are connected along a main axis x – referred to as the direction of propagation. Also, these substructures are assumed to be discretized by means of a similar FE model containing a similar number n of DOFs over its left and right boundaries. The FE models of several kinds of periodic structures – namely, waveguides – and related substructures are depicted in Figure 1. In the present study, these waveguides are supposed to be elastic, dissipative (considering a loss factor η) and subjected to harmonic disturbance under frequency $\omega/2\pi$ (ω being the pulsation).

Figure 1

5

Within the WFE method, the waves traveling along the $x-$direction (see above) of any waveguide are computed using the FE model of the related substructure. Clearly, this requires the mass and stiffness matrices of the substructure to be known, e.g. using a commercial FE software. Also, the dynamic stiffness matrix of the substructure, condensed on its left and right boundaries, has to be expressed. The strategy for computing the waves is to consider a state vector representation [14] for linking the vectors of displacements / forces between the left (or right) boundaries of two adjacent substructures k and $k-1$. In the frequency domain, this relationship is expressed in terms of a $2n \times 2n$ symplectic matrix $\mathbf{S}$ as [1]

$$\mathbf{u}^{(k)} = \mathbf{S}\mathbf{u}^{(k-1)} \qquad k = 2, \ldots, N+1, \tag{1}$$

where N is the number of substructures considered along the whole waveguide, while $N+1$ is to be understood as the number of substructure boundaries (say, the coupling interfaces between the substructures as well as the two limiting boundaries of the waveguide). These substructure boundaries are depicted in Figure 2. In Eq. (1), $\mathbf{u}$ refers to a $2n \times 1$ state vector expressed as

$$\mathbf{u} = \begin{bmatrix} \mathbf{q} \\ \pm\mathbf{F} \end{bmatrix}, \tag{2}$$

where $\mathbf{q}$ and $\mathbf{F}$ are the vectors of displacements and forces, respectively, over the left or right boundary of the substructures. The sign ahead $\mathbf{F}$ results from the convention made for expressing the forces on the left or right boundaries of the substructures. It is worth emphasizing that the matrix $\mathbf{S}$ is expressed from the condensed dynamic stiffness matrix of the substructure (see e.g. ref. [15] for further details).

The computation of the waves traveling along the $x-$direction follows directly from Bloch's theorem [16]:

Bloch's theorem: a simple statement. *Let* $\mathbf{S}$ *be* $d-$ *periodic, thus* $\mathbf{u}^{(k)}$ *can be expanded as* $\sum_j Q_j^{(k)} \mathbf{\Phi}_j$ *where* $Q_j^{(k)} = \mathrm{e}^{-\mathrm{i}\beta_j d} Q_j^{(k-1)} \ \forall j.$

It is worth recalling that d is the length (i.e. along the $x-$direction) of any substructure used for describing the whole waveguide. Bloch's theorem particularly states that the eigenvalues of $\mathbf{S}$ – namely $\{\mu_j\}_j$ – can be expressed as $\{\mathrm{e}^{-\mathrm{i}\beta_j d}\}_j$, where $\{\beta_j\}_j$ have the meaning of wavenumbers. Regarding these, the waves can be classified as propagating (i.e. the imaginary parts of the wavenumbers are close to zero), evanescent (i.e. the real parts of the wavenumbers are close to zero) or complex (i.e. the real and imaginary parts of the wavenumbers are of the same order). On the other hand, the terms $\{\mathbf{\Phi}_j\}_j$ are the eigenvectors of $\mathbf{S}$ – also known as the wave shapes –, which relate the spatial distribution of the displacements and forces over the substructure boundaries. Several illustrations of wave shapes are brought in ref. [1], considering the waveguides depicted in Figure 1. For example, considering beam-like structures, the wave shapes are to be understood as particular spatial distributions of the displacements and internal forces over the cross-section, "traveling" at different velocities along the waveguide. In ref. [1], it is shown that the WFE method is well suited for describing the classic wave shapes (i.e. longitudinal, torsional, flexural, shearing) as well as many other high order wave shapes (with an oscillating spatial behavior over the cross-section) which are useful to capture the structure dynamics in the MF range.

The set of terms $\{(\mu_j, \mathbf{\Phi}_j)\}_j$, as well as $\{\mathbf{\Phi}_j\}_j$, are usually called the wave modes. They are twice as many as the number of DOFs contained over the left or right substructure boundary, i.e. $2n$. Considering that the matrix $\mathbf{S}$ is symplectic (see above) yields $\{(\mu_j, \mathbf{\Phi}_j)\}_j$ to be split into n incident and n reflected wave modes, say n waves traveling towards and n waves traveling outward the right

7

(or left) boundary of the waveguide. These incident and reflected wave modes are denoted as $\{(\mu_j^{\text{inc}}, \boldsymbol{\Phi}_j^{\text{inc}})\}_j$ and $\{(\mu_j^{\text{ref}}, \boldsymbol{\Phi}_j^{\text{ref}})\}_j$; they are usually defined such that $|\mu_j^{\text{inc}}| < 1$ and $|\mu_j^{\text{ref}}| > 1$ $\forall j$ (such a consideration arises from the fact that $\mathbf{S}$ is a symplectic matrix, i.e. its eigenvalues come in pairs as $(\mu, 1/\mu)$).

Otherwise, Bloch's theorem also implies that any state vector $\mathbf{u}^{(k)}$ – which relates the vectors of displacements $\mathbf{q}^{(k)}$ and forces $\mathbf{F}^{(k)}$ at the substructure boundary k ($k = 1, \ldots, N + 1$), along the waveguide – can be expanded in terms of wave modes $\{\boldsymbol{\Phi}_j\}_j$ and wave amplitudes $\{Q_j\}_j$. The wave mode expansions are expressed as

$$\mathbf{q}^{(k)} = \boldsymbol{\Phi}_{\mathbf{q}}^{\text{inc}}\mathbf{Q}^{\text{inc}(k)} + \boldsymbol{\Phi}_{\mathbf{q}}^{\text{ref}}\mathbf{Q}^{\text{ref}(k)} \qquad k = 1, \ldots, N + 1, \tag{3}$$

$$\pm\mathbf{F}^{(k)} = \boldsymbol{\Phi}_{\mathbf{F}}^{\text{inc}}\mathbf{Q}^{\text{inc}(k)} + \boldsymbol{\Phi}_{\mathbf{F}}^{\text{ref}}\mathbf{Q}^{\text{ref}(k)} \qquad k = 1, \ldots, N + 1, \tag{4}$$

where $\boldsymbol{\Phi}_{\mathbf{q}}^{\text{inc}}$, $\boldsymbol{\Phi}_{\mathbf{q}}^{\text{ref}}$, $\boldsymbol{\Phi}_{\mathbf{F}}^{\text{inc}}$ and $\boldsymbol{\Phi}_{\mathbf{F}}^{\text{ref}}$ are square $n \times n$ matrices constituted from the displacement and force components of the incident and reflected wave shapes; also, $\mathbf{Q}^{\text{inc}(k)}$ and $\mathbf{Q}^{\text{ref}(k)}$ are $n \times 1$ vectors of wave amplitudes, whose variation along the waveguide is expressed as [1]

$$\mathbf{Q}^{\text{inc}(k)} = \boldsymbol{\mu}^{k-1}\mathbf{Q}^{\text{inc}(1)} \qquad k = 1, \ldots, N + 1, \tag{5}$$

$$\mathbf{Q}^{\text{ref}(k)} = \boldsymbol{\mu}^{-(k-1)}\mathbf{Q}^{\text{ref}(1)} \qquad k = 1, \ldots, N + 1. \tag{6}$$

Here, $\boldsymbol{\mu}$ is defined as $\boldsymbol{\mu} = \texttt{diag}\{\mu_j^{\text{inc}}\}_j$. Considering that $|\mu_j^{\text{inc}}| < 1$ $\forall j$ (see above) results in $||\boldsymbol{\mu}|| < 1$ ($||.||$ being the $2-$norm).

2.2. Conventions

For any waveguide, let us denote as $\boldsymbol{\Phi}^{\text{inc}}$ and $\boldsymbol{\Phi}^{\text{ref}}$ the matrices of incident and reflected wave modes defined as

$$\boldsymbol{\Phi}^{\text{inc}} = \begin{bmatrix} \boldsymbol{\Phi}_{\mathbf{q}}^{\text{inc}} \\ \boldsymbol{\Phi}_{\mathbf{F}}^{\text{inc}} \end{bmatrix} \quad , \quad \boldsymbol{\Phi}^{\text{ref}} = \begin{bmatrix} \boldsymbol{\Phi}_{\mathbf{q}}^{\text{ref}} \\ \boldsymbol{\Phi}_{\mathbf{F}}^{\text{ref}} \end{bmatrix}, \tag{7}$$

where the matrices $\mathbf{\Phi}_q^{\texttt{inc}}$, $\mathbf{\Phi}_q^{\texttt{ref}}$, $\mathbf{\Phi}_F^{\texttt{inc}}$ and $\mathbf{\Phi}_F^{\texttt{ref}}$ have been defined in Section 2.1. It is worth recalling that the vectors of wave amplitudes are denoted as $\mathbf{Q}^{\texttt{inc}(k)}$ and $\mathbf{Q}^{\texttt{ref}(k)}$.

As a convention, these notations for matrices and vectors will be used throughout the paper to denote the wave modes that are incident to and reflected by the *right boundary* of the waveguide (cf. Figure 2). In contrast, considering the *left boundary* of the waveguide, it is proposed to denote the matrices of incident and reflected wave modes as $\mathbf{\Phi}^{\texttt{inc}\star}$ and $\mathbf{\Phi}^{\texttt{ref}\star}$, and to denote the related vectors of wave amplitudes as $\mathbf{Q}^{\texttt{inc}\star(k)}$ and $\mathbf{Q}^{\texttt{ref}\star(k)}$. These matrix and vector terms are simply expressed as

$$\mathbf{\Phi}^{\texttt{inc}\star} = \mathbf{\Phi}^{\texttt{ref}} \quad , \quad \mathbf{\Phi}^{\texttt{ref}\star} = \mathbf{\Phi}^{\texttt{inc}}, \tag{8}$$

$$\mathbf{Q}^{\texttt{inc}\star(k)} = \mathbf{Q}^{\texttt{ref}(k)} \quad , \quad \mathbf{Q}^{\texttt{ref}\star(k)} = \mathbf{Q}^{\texttt{inc}(k)} \qquad k = 1, \ldots, N+1. \tag{9}$$

Such conventions involving the right and left boundaries of the waveguide are depicted in Figure 2. They are introduced here as a means to clarify the concept behind incident and reflected wave modes. Also, the following notations are introduced as a means to simplify the subsequent formulations made in the paper:

$$\mathbf{Q}^{\texttt{inc}} = \mathbf{Q}^{\texttt{inc}(N+1)} \quad , \quad \mathbf{Q}^{\texttt{ref}} = \mathbf{Q}^{\texttt{ref}(N+1)}, \tag{10}$$

$$\mathbf{Q}^{\texttt{inc}\star} = \mathbf{Q}^{\texttt{inc}\star(1)} \quad , \quad \mathbf{Q}^{\texttt{ref}\star} = \mathbf{Q}^{\texttt{ref}\star(1)}, \tag{11}$$

where $\{\mathbf{Q}^{\texttt{inc}}, \mathbf{Q}^{\texttt{ref}}\}$ are to be understood as the vectors of wave amplitudes expressed at the right boundary of the waveguide (i.e. the substructure boundary $N+1$), while $\{\mathbf{Q}^{\texttt{inc}\star}, \mathbf{Q}^{\texttt{ref}\star}\}$ are the vectors of wave amplitudes expressed at the left boundary of the waveguide (i.e. the substructure boundary 1). The meaning of substructure boundaries is clarified in Figure 2. Using the aforementioned notations enables the boundary conditions of the waveguide to be simply expressed.

For instance, Neumann or Dirichlet boundary conditions are readily written as [17]

$$\mathbf{Q}^{\texttt{ref}} = \mathbb{C}\mathbf{Q}^{\texttt{inc}} + \mathbb{F} \quad , \quad \mathbf{Q}^{\texttt{ref}\star} = \mathbb{C}^{\star}\mathbf{Q}^{\texttt{inc}\star} + \mathbb{F}^{\star}, \tag{12}$$

where $\mathbb{C}$ and $\mathbb{C}^{\star}$ are $n \times n$ matrices whose components refer to the reflection coefficients, while $\mathbb{F}$ and $\mathbb{F}^{\star}$ are $n \times 1$ vectors whose components play the role of excitation sources (expressions for those matrices and vectors directly follows from the wave mode expansions (3) and (4)). Also, Eq. (12) can be applied to describe coupling conditions, e.g. considering two waveguides 1 and 2 connected with an elastic junction (cf. Figure 2(d)). In this case, the matrix $\mathbb{C}$ can be partitioned as [1]

$$\mathbb{C} = \begin{bmatrix} \mathbb{C}_{11} & \mathbb{C}_{12} \\ \mathbb{C}_{21} & \mathbb{C}_{22} \end{bmatrix}, \tag{13}$$

where the components of matrices $\mathbb{C}_{11}$ and $\mathbb{C}_{22}$ denote the reflection coefficients of the wave modes traveling in waveguides 1 and 2 towards the coupling junction, while the components of matrices $\mathbb{C}_{12}$ and $\mathbb{C}_{21}$ denote the transmission coefficients of these wave modes through the coupling junction.

It must be noted that, according to Eqs. (5) and (6), the vectors of wave amplitudes $\{\mathbf{Q}^{\texttt{inc}}, \mathbf{Q}^{\texttt{ref}}\}$ and $\{\mathbf{Q}^{\texttt{inc}\star}, \mathbf{Q}^{\texttt{ref}\star}\}$ are linked as

$$\mathbf{Q}^{\texttt{inc}} = \boldsymbol{\mu}^{N}\mathbf{Q}^{\texttt{ref}\star} \quad , \quad \mathbf{Q}^{\texttt{inc}\star} = \boldsymbol{\mu}^{N}\mathbf{Q}^{\texttt{ref}}. \tag{14}$$

Figure 2

2.3. *Forced response computation*

The strategy for computing the forced response of waveguides has been proposed in ref. [1]. In brief, considering a single waveguide subjected to Neumann

or Dirichlet boundary conditions (cf. Figure 1(a-c)), it can be shown that the vectors of wave amplitudes $\mathbf{Q}^{\texttt{ref}}$ and $\mathbf{Q}^{\texttt{ref}\star}$ (cf. Eq. (12)) are the solutions of the following $2n \times 2n$ matrix system:

$$
\begin{bmatrix} \mathbf{I}_n & -\mathbb{C}^\star \boldsymbol{\mu}^N \\ -\mathbb{C}\boldsymbol{\mu}^N & \mathbf{I}_n \end{bmatrix} \begin{bmatrix} \mathbf{Q}^{\texttt{ref}\star} \\ \mathbf{Q}^{\texttt{ref}} \end{bmatrix} = \begin{bmatrix} \mathbb{F}^\star \\ \mathbb{F} \end{bmatrix}.
\tag{15}
$$

The computation of the vectors of displacements $\mathbf{q}^{(k)}$ and forces $\mathbf{F}^{(k)}$ follows from the wave mode expansions (3) and (4).

In contrast, considering two waveguides connected through an elastic junction (cf. Figure 1(d)) yields the following matrix system to be considered:

$$
\left[\begin{array}{cc|cc} \mathbf{I}_{n_1} & -\mathbb{C}_1^\star \boldsymbol{\mu}_1^{N_1} & \mathbf{0} & \mathbf{0} \\ -\mathbb{C}_{11}\boldsymbol{\mu}_1^{N_1} & \mathbf{I}_{n_1} & \mathbf{0} & -\mathbb{C}_{12}\boldsymbol{\mu}_2^{N_2} \\ \hline -\mathbb{C}_{21}\boldsymbol{\mu}_1^{N_1} & \mathbf{0} & \mathbf{I}_{n_2} & -\mathbb{C}_{22}\boldsymbol{\mu}_2^{N_2} \\ \mathbf{0} & \mathbf{0} & -\mathbb{C}_2^\star \boldsymbol{\mu}_2^{N_2} & \mathbf{I}_{n_2} \end{array} \right] \left[\begin{array}{c} \mathbf{Q}_1^{\texttt{ref}\star} \\ \mathbf{Q}_1^{\texttt{ref}} \\ \hline \mathbf{Q}_2^{\texttt{ref}} \\ \mathbf{Q}_2^{\texttt{ref}\star} \end{array} \right] = \left[\begin{array}{c} \mathbb{F}_1^\star \\ \mathbf{0} \\ \hline \mathbf{0} \\ \mathbb{F}_2^\star \end{array} \right],
\tag{16}
$$

where the subscripts 1 and 2 refer to vector and matrix terms associated to waveguides 1 and 2, respectively; otherwise, $\mathbb{C}_1^\star$ and $\mathbb{C}_2^\star$ are two matrices of reflection coefficients which describe the waveguide boundaries that are not involved by the coupling conditions. Considering Eq. (16), the size of the matrix system is $2(n_1 + n_2) \times 2(n_1 + n_2)$, where n_1 (resp. n_2) is the number of DOFs used for discretizing the left or right boundary of any substructure considered in waveguide 1 (resp. waveguide 2).

2.4. Concept of model reduction

2.4.1. Some general notations and properties related to matrix norms

The proposed model reduction strategy mainly focuses on the use of matrix norms. As a preliminary step, it is proposed to clarify the following notations and properties that are used throughout the paper:

- The notation $||\mathbf{X}||$ refers to the $2-$norm of a matrix or a vector $\mathbf{X}$. The consistency property of the $2-$norm means that $||\mathbf{AB}|| \leq ||\mathbf{A}||\,||\mathbf{B}||$ for arbitrary $p \times q$ matrix $\mathbf{A}$ and $q \times r$ matrix $\mathbf{B}$;

- A rectangular $n \times m$ ($m \leq n$) real matrix $\mathbf{C}$ will be called orthogonal or unitary in the sense that $\mathbf{C}^T\mathbf{C} = \mathbf{I}_m$. The $2-$norm will be said to be unitarily invariant in the sense that $||\mathbf{CD}|| = ||\mathbf{D}||$ for any $m \times p$ matrix $\mathbf{D}$;

- The notation $\rho(\mathbf{E})$ refers to the spectral radius of a square matrix $\mathbf{E}$, with the property that $\rho(\mathbf{E}) \leq ||\mathbf{E}||$.

Apart from this, the notation $\mathbf{A}^T$ denotes the transpose of a matrix $\mathbf{A}$, while the notation $\mathbf{I}_n$ denotes the $n \times n$ identity matrix.

2.4.2. Error norms

Within the WFE framework, the displacements and internal forces of any waveguide are usually approximated by means of a reduced basis $\{\widetilde{\mathbf{\Phi}}_j\}_{j=1,\ldots,2m}$ containing a same number m ($m \leq n$) of incident and reflected wave modes. The related vectors of wave amplitudes are obtained by considering the matrix formulations (15) or (16). The reduced basis is extracted from the full wave basis $\{\mathbf{\Phi}_j\}_{j=1,\ldots,2n}$ already depicted in Section 2.1. Considering such a reduced basis yields the wave expansions to be expressed as

$$\widetilde{\mathbf{q}}^{(k)} = \widetilde{\mathbf{\Phi}}_{\mathtt{q}}^{\mathtt{inc}}\widetilde{\mathbf{Q}}^{\mathtt{inc}(k)} + \widetilde{\mathbf{\Phi}}_{\mathtt{q}}^{\mathtt{ref}}\widetilde{\mathbf{Q}}^{\mathtt{ref}(k)} \qquad k = 1, \ldots, N+1, \tag{17}$$

$$\pm\widetilde{\mathbf{F}}^{(k)} = \widetilde{\mathbf{\Phi}}_{\mathtt{F}}^{\mathtt{inc}}\widetilde{\mathbf{Q}}^{\mathtt{inc}(k)} + \widetilde{\mathbf{\Phi}}_{\mathtt{F}}^{\mathtt{ref}}\widetilde{\mathbf{Q}}^{\mathtt{ref}(k)} \qquad k = 1, \ldots, N+1, \tag{18}$$

where $\widetilde{\mathbf{\Phi}}_{\mathtt{q}}^{\mathtt{inc}}$, $\widetilde{\mathbf{\Phi}}_{\mathtt{q}}^{\mathtt{ref}}$, $\widetilde{\mathbf{\Phi}}_{\mathtt{F}}^{\mathtt{inc}}$ and $\widetilde{\mathbf{\Phi}}_{\mathtt{F}}^{\mathtt{ref}}$ are $n \times m$ matrices constituted from the displacement and force components of the incident and reflected wave modes; also,

$\widetilde{\mathbf{Q}}^{\mathtt{inc}(k)}$ and $\widetilde{\mathbf{Q}}^{\mathtt{ref}(k)}$ are the $m \times 1$ related vectors of wave amplitudes, whose variations along the waveguide follow from Eqs. (5) and (6) as

$$\widetilde{\mathbf{Q}}^{\mathtt{inc}(k)} = \widetilde{\boldsymbol{\mu}}^{k-1} \widetilde{\mathbf{Q}}^{\mathtt{inc}(1)} \qquad k = 1, \ldots, N+1, \tag{19}$$

$$\widetilde{\mathbf{Q}}^{\mathtt{ref}(k)} = \widetilde{\boldsymbol{\mu}}^{-(k-1)} \widetilde{\mathbf{Q}}^{\mathtt{ref}(1)} \qquad k = 1, \ldots, N+1, \tag{20}$$

where $\widetilde{\boldsymbol{\mu}} = \mathtt{diag}\{\widetilde{\mu}_j^{\mathtt{inc}}\}_j$, $\{\widetilde{\mu}_j^{\mathtt{inc}}\}_j \subseteq \{\mu_j^{\mathtt{inc}}\}_j$ being the wave parameters associated to the wave modes $\{\widetilde{\boldsymbol{\Phi}}_j\}_j$ (cf. Section 2.1); it is worth noting that $||\widetilde{\boldsymbol{\mu}}|| < 1$, because $||\widetilde{\boldsymbol{\mu}}|| \leq ||\boldsymbol{\mu}||$ (it is worth recalling that $\boldsymbol{\mu} = \mathtt{diag}\{\mu_j^{\mathtt{inc}}\}_j$ while $\{\widetilde{\mu}_j^{\mathtt{inc}}\}_j \subseteq \{\mu_j^{\mathtt{inc}}\}_j$) and $||\boldsymbol{\mu}|| < 1$ (see below Eq. (6)).

The idea behind the technique of model order reduction (MOR) is to approximate the vectors of displacements and forces over any substructure boundary k as $\mathbf{q}^{(k)} \approx \widetilde{\mathbf{q}}^{(k)}$ and $\mathbf{F}^{(k)} \approx \widetilde{\mathbf{F}}^{(k)}$ with reasonable accuracy while using a reduced wave basis of minimum size $2m$. Investigating these vectors of displacements and forces by means of a reduced wave basis (instead of the full basis) enables the computation of the forced responses to be done using matrix systems of small sizes (cf. e.g. Eq. (15)), i.e. $2m \times 2m$ instead of $2n \times 2n$. Such a MOR strategy addresses the minimization of the norms $||\widetilde{\mathbf{q}}^{(k)} - \mathbf{q}^{(k)}||$ and $||\widetilde{\mathbf{F}}^{(k)} - \mathbf{F}^{(k)}||$, whose derivation is proposed hereafter.

Let us introduce the $m \times n$ incidence matrix $\widetilde{\mathcal{L}}$ defined as $\widetilde{\boldsymbol{\Phi}}_{\mathtt{q}}^{\mathtt{inc}} = \boldsymbol{\Phi}_{\mathtt{q}}^{\mathtt{inc}} \widetilde{\mathcal{L}}^T$, $\widetilde{\boldsymbol{\Phi}}_{\mathtt{q}}^{\mathtt{ref}} = \boldsymbol{\Phi}_{\mathtt{q}}^{\mathtt{ref}} \widetilde{\mathcal{L}}^T$, $\widetilde{\boldsymbol{\Phi}}_{\mathtt{F}}^{\mathtt{inc}} = \boldsymbol{\Phi}_{\mathtt{F}}^{\mathtt{inc}} \widetilde{\mathcal{L}}^T$, $\widetilde{\boldsymbol{\Phi}}_{\mathtt{F}}^{\mathtt{ref}} = \boldsymbol{\Phi}_{\mathtt{F}}^{\mathtt{ref}} \widetilde{\mathcal{L}}^T$, where $\widetilde{\mathcal{L}}^T$ is real orthogonal (i.e. it is unitary). Clearly speaking, the matrix $\widetilde{\mathcal{L}}$ is constructed so that each of its rows contains a single 1 and 0 elsewhere. Considering such an incidence matrix $\widetilde{\mathcal{L}}$ yields the errors $\widetilde{\mathbf{q}}^{(k)} - \mathbf{q}^{(k)}$ and $\widetilde{\mathbf{F}}^{(k)} - \mathbf{F}^{(k)}$ to be expressed as

$$\widetilde{\mathbf{q}}^{(k)} - \mathbf{q}^{(k)} = \boldsymbol{\Phi}_{\mathtt{q}}^{\mathtt{inc}} \Delta \mathbf{Q}^{\mathtt{inc}(k)} + \boldsymbol{\Phi}_{\mathtt{q}}^{\mathtt{ref}} \Delta \mathbf{Q}^{\mathtt{ref}(k)} \qquad k = 1, \ldots, N+1, \tag{21}$$

$$\pm(\widetilde{\mathbf{F}}^{(k)} - \mathbf{F}^{(k)}) = \boldsymbol{\Phi}_{\mathtt{F}}^{\mathtt{inc}} \Delta \mathbf{Q}^{\mathtt{inc}(k)} + \boldsymbol{\Phi}_{\mathtt{F}}^{\mathtt{ref}} \Delta \mathbf{Q}^{\mathtt{ref}(k)} \qquad k = 1, \ldots, N+1, \tag{22}$$

where $\Delta\mathbf{Q}^{\mathtt{inc}(k)}$ and $\Delta\mathbf{Q}^{\mathtt{ref}(k)}$ are expressed of the form

$$\Delta\mathbf{Q} = \widetilde{\mathcal{L}}^{T}\widetilde{\mathbf{Q}} - \mathbf{Q}. \tag{23}$$

From the consistency property of the $2-$norm (see Section 2.4.1), it turns out from Eqs. (21) and (22) that $||\widetilde{\mathbf{q}}^{(k)} - \mathbf{q}^{(k)}||$ and $||\widetilde{\mathbf{F}}^{(k)} - \mathbf{F}^{(k)}||$ are bounded as

$$||\widetilde{\mathbf{q}}^{(k)} - \mathbf{q}^{(k)}|| \leq ||\mathbf{\Phi}_{\mathtt{q}}^{\mathtt{inc}}||\,||\Delta\mathbf{Q}^{\mathtt{inc}(k)}|| + ||\mathbf{\Phi}_{\mathtt{q}}^{\mathtt{ref}}||\,||\Delta\mathbf{Q}^{\mathtt{ref}(k)}||$$
$$k = 1, \ldots, N+1, \tag{24}$$

$$||\widetilde{\mathbf{F}}^{(k)} - \mathbf{F}^{(k)}|| \leq ||\mathbf{\Phi}_{\mathtt{F}}^{\mathtt{inc}}||\,||\Delta\mathbf{Q}^{\mathtt{inc}(k)}|| + ||\mathbf{\Phi}_{\mathtt{F}}^{\mathtt{ref}}||\,||\Delta\mathbf{Q}^{\mathtt{ref}(k)}||$$
$$k = 1, \ldots, N+1. \tag{25}$$

It is worth emphasizing that the matrices $\mathbf{\Phi}_{\mathtt{q}}^{\mathtt{inc}}$ and $\mathbf{\Phi}_{\mathtt{F}}^{\mathtt{inc}}$, as well as the matrices $\mathbf{\Phi}_{\mathtt{q}}^{\mathtt{ref}}$ and $\mathbf{\Phi}_{\mathtt{F}}^{\mathtt{ref}}$, are linked as $\mathbf{\Phi}_{\mathtt{q}}^{\mathtt{ref}} = \mathcal{R}\mathbf{\Phi}_{\mathtt{q}}^{\mathtt{inc}}$ and $\mathbf{\Phi}_{\mathtt{F}}^{\mathtt{ref}} = -\mathcal{R}\mathbf{\Phi}_{\mathtt{F}}^{\mathtt{inc}}$, where $\mathcal{R}$ is a diagonal symmetry transformation matrix [1], i.e. which is unitary. This yields $||\mathbf{\Phi}_{\mathtt{q}}^{\mathtt{ref}}|| = ||\mathbf{\Phi}_{\mathtt{q}}^{\mathtt{inc}}||$ and $||\mathbf{\Phi}_{\mathtt{F}}^{\mathtt{ref}}|| = ||\mathbf{\Phi}_{\mathtt{F}}^{\mathtt{inc}}||$, because the $2-$norm is unitarily invariant (see Section 2.4.1). As a result, considering Eqs. (24) and (25) yields

$$||\widetilde{\mathbf{q}}^{(k)} - \mathbf{q}^{(k)}|| \leq ||\mathbf{\Phi}_{\mathtt{q}}^{\mathtt{inc}}|| \left(||\Delta\mathbf{Q}^{\mathtt{inc}(k)}|| + ||\Delta\mathbf{Q}^{\mathtt{ref}(k)}|| \right)$$
$$k = 1, \ldots, N+1, \tag{26}$$

$$||\widetilde{\mathbf{F}}^{(k)} - \mathbf{F}^{(k)}|| \leq ||\mathbf{\Phi}_{\mathtt{F}}^{\mathtt{inc}}|| \left(||\Delta\mathbf{Q}^{\mathtt{inc}(k)}|| + ||\Delta\mathbf{Q}^{\mathtt{ref}(k)}|| \right)$$
$$k = 1, \ldots, N+1. \tag{27}$$

To summarize, the issue behind the reduction of the norms $||\widetilde{\mathbf{q}}^{(k)} - \mathbf{q}^{(k)}||$ and $||\widetilde{\mathbf{F}}^{(k)} - \mathbf{F}^{(k)}||$ is to reduce the term $||\Delta\mathbf{Q}^{\mathtt{inc}(k)}|| + ||\Delta\mathbf{Q}^{\mathtt{ref}(k)}||$, i.e. to reduce the error norms $||\Delta\mathbf{Q}^{\mathtt{inc}(k)}||$ and $||\Delta\mathbf{Q}^{\mathtt{ref}(k)}||$. Bounds of these error norms are expressed as follows.

Let us introduce the $(n - m) \times n$ incidence matrix $\mathcal{L}_{\mathtt{r}}$ such that $\mathcal{L}_{\mathtt{r}}^T$ is unitary and $\mathcal{L}_{\mathtt{r}}^T \mathcal{L}_{\mathtt{r}} + \widetilde{\mathcal{L}}^T \widetilde{\mathcal{L}} = \mathbf{I}_n$. The expected matrix $\mathcal{L}_{\mathtt{r}}$ is defined so that each of its rows contains a single 1 (whose location is actually imposed by the constraint $\mathcal{L}_{\mathtt{r}}^T \mathcal{L}_{\mathtt{r}} + \widetilde{\mathcal{L}}^T \widetilde{\mathcal{L}} = \mathbf{I}_n$) and 0 elsewhere.

Proposition 1. *The error norms $||\Delta \mathbf{Q}^{\mathtt{inc}(k)}||$ and $||\Delta \mathbf{Q}^{\mathtt{ref}(k)}||$ are bounded as*

$$||\Delta \mathbf{Q}|| \leq ||\widetilde{\mathbf{Q}} - \widetilde{\mathcal{L}}\mathbf{Q}|| + ||\mathcal{L}_{\mathtt{r}}\mathbf{Q}||. \tag{28}$$

Proof. Let us denote as $\mathbf{Q}$ either $\mathbf{Q}^{\mathtt{inc}(k)}$ or $\mathbf{Q}^{\mathtt{ref}(k)}$. Considering that $\mathbf{Q} = \widetilde{\mathcal{L}}^T \widetilde{\mathcal{L}} \mathbf{Q} + (\mathbf{I}_n - \widetilde{\mathcal{L}}^T \widetilde{\mathcal{L}})\mathbf{Q}$ and using the fact that $\mathcal{L}_{\mathtt{r}}^T \mathcal{L}_{\mathtt{r}} + \widetilde{\mathcal{L}}^T \widetilde{\mathcal{L}} = \mathbf{I}_n$ yields

$$\mathbf{Q} = \widetilde{\mathcal{L}}^T \widetilde{\mathcal{L}} \mathbf{Q} + \mathcal{L}_{\mathtt{r}}^T \mathcal{L}_{\mathtt{r}} \mathbf{Q}. \tag{29}$$

According to Eq. (23), $\Delta \mathbf{Q}$ is expressed as $\widetilde{\mathcal{L}}^T \widetilde{\mathbf{Q}} - \mathbf{Q}$ which, according to Eq. (29), gives

$$\Delta \mathbf{Q} = \widetilde{\mathcal{L}}^T (\widetilde{\mathbf{Q}} - \widetilde{\mathcal{L}}\mathbf{Q}) - \mathcal{L}_{\mathtt{r}}^T \mathcal{L}_{\mathtt{r}} \mathbf{Q}. \tag{30}$$

It follows that $||\Delta \mathbf{Q}||$ is bounded as

$$||\Delta \mathbf{Q}|| \leq ||\widetilde{\mathcal{L}}^T (\widetilde{\mathbf{Q}} - \widetilde{\mathcal{L}}\mathbf{Q})|| + ||\mathcal{L}_{\mathtt{r}}^T \mathcal{L}_{\mathtt{r}} \mathbf{Q}||. \tag{31}$$

Considering that $\widetilde{\mathcal{L}}^T$ and $\mathcal{L}_{\mathtt{r}}^T$ are unitary (by definition) yields $||\widetilde{\mathcal{L}}^T (\widetilde{\mathbf{Q}} - \widetilde{\mathcal{L}}\mathbf{Q})|| = ||\widetilde{\mathbf{Q}} - \widetilde{\mathcal{L}}\mathbf{Q}||$ and $||\mathcal{L}_{\mathtt{r}}^T \mathcal{L}_{\mathtt{r}} \mathbf{Q}|| = ||\mathcal{L}_{\mathtt{r}}\mathbf{Q}||$ (since the $2-$norm is unitarily invariant). Taking into account these results in Eq. (31) leads to Eq. (28), as expected. $\quad\square$

In Eq. (28), $\widetilde{\mathcal{L}}\mathbf{Q}$ and $\widetilde{\mathbf{Q}}$ are the vectors of wave amplitudes associated to the retained wave modes $\{\widetilde{\mathbf{\Phi}}_j\}_j$, respectively computed (cf. Eqs. (15) and (16)) using

the full wave basis $\{\boldsymbol{\Phi}_j\}_j$ and the reduced wave basis $\{\widetilde{\boldsymbol{\Phi}}_j\}_j$. On the other hand, $\mathcal{L}_{\mathbf{r}}\mathbf{Q}$ is the vector of wave amplitudes associated to the residual wave modes – i.e. which are not included in the reduced basis $\{\widetilde{\boldsymbol{\Phi}}_j\}_j$ – computed using the full wave basis $\{\boldsymbol{\Phi}_j\}_j$. According to Proposition 1, the error $||\Delta\mathbf{Q}||$ involved by the reduction of the wave basis reveals two aspects. One is linked to the norm $||\widetilde{\mathbf{Q}} - \widetilde{\mathcal{L}}\mathbf{Q}||$ which addresses the accuracy of the reduced model to compute the wave amplitudes of the retained wave modes; the other one is linked to the norm $||\mathcal{L}_{\mathbf{r}}\mathbf{Q}||$ which addresses the error involved when the residual wave modes are omitted in the WFE matrix formulation (cf. Eqs. (15) and (16)).

To summarize, the model reduction strategy can be understood as seeking a wave basis $\{\widetilde{\boldsymbol{\Phi}}_j\}_j$ with optimal reduced size for minimizing the term $||\widetilde{\mathbf{Q}} - \widetilde{\mathcal{L}}\mathbf{Q}|| + ||\mathcal{L}_{\mathbf{r}}\mathbf{Q}||$. Such an issue is addressed in the next section, considering the case of single waveguides subjected to Neumann and Dirichlet boundary conditions (the case of coupled waveguides will be discussed in Section 4).

3. MOR strategy

3.1. Preliminary comments

Let us consider a single waveguide involving Neumann / Dirichlet boundary conditions over its left and right ends (cf. for instance Figures 1(a-c)). Eq. (28) expresses a bound for the error norm $||\Delta\mathbf{Q}||$, i.e. either $||\Delta\mathbf{Q}^{\mathtt{inc}(k)}||$ or $||\Delta\mathbf{Q}^{\mathtt{ref}(k)}||$ (it is worth recalling that these norms are to be considered for every substructure boundary k ($k = 1, \ldots, N + 1$)). According to Eq. (9), the vector of wave amplitudes $\mathbf{Q}^{\mathtt{ref}(k)}$ writes as $\mathbf{Q}^{\mathtt{inc}\star(k)}$, say it can be deduced from the vector of wave amplitudes $\mathbf{Q}^{\mathtt{inc}(k)}$ by considering the following substitutions $\mathbb{C} \to \mathbb{C}^\star$ and $\mathbb{F} \to \mathbb{F}^\star$ (cf. Eq. (12)). In other words, the minimization prob-

16

lem of $||\Delta \mathbf{Q}^{\text{inc}(k)}|| + ||\Delta \mathbf{Q}^{\text{ref}(k)}||$ (see Section 2.4.2) can be deduced from the consideration of the error norm $||\Delta \mathbf{Q}^{\text{inc}(k)}||$ only, the latter being bounded as (cf. Proposition 1)

$$||\Delta \mathbf{Q}^{\text{inc}(k)}|| \leq ||\widetilde{\mathbf{Q}}^{\text{inc}(k)} - \widetilde{\mathcal{L}}\mathbf{Q}^{\text{inc}(k)}|| + ||\mathcal{L}_{\mathbf{r}}\mathbf{Q}^{\text{inc}(k)}||$$

$$k = 1, \ldots, N+1. \quad (32)$$

In order to quantify the contribution of any wave mode for reducing the bound provided by Eq. (32), it is proposed to derive the vectors of wave amplitudes $\mathbf{Q}^{\text{inc}(k)}$ and $\widetilde{\mathbf{Q}}^{\text{inc}(k)}$ by means of the wave parameters $\{\mu_j\}_j$ and $\{\widetilde{\mu}_j\}_j$ (see Section 2), as well as the waveguide boundary conditions (cf. Eq. (12)). The key idea is to consider a finite number of forward and backward passings of waves along the waveguide for expressing $\mathbf{Q}^{\text{inc}(k)}$ and $\widetilde{\mathbf{Q}}^{\text{inc}(k)}$. Such a strategy is proposed hereafter.

3.2. Expression of the vectors of wave amplitudes

Considering Eq. (5), the vector of wave amplitudes $\mathbf{Q}^{\text{inc}(k)}$ is expressed as $\boldsymbol{\mu}^{k-1}\mathbf{Q}^{\text{inc}(1)}$. Invoking Eqs. (9) and (11) yields $\mathbf{Q}^{\text{inc}(1)} = \mathbf{Q}^{\text{ref}\star}$, while invoking the boundary conditions (12) leads to

$$\mathbf{Q}^{\text{inc}(k)} = \boldsymbol{\mu}^{k-1}\left(\mathbb{C}^{\star}\mathbf{Q}^{\text{inc}\star} + \mathbb{F}^{\star}\right) \qquad k = 1, \ldots, N+1. \quad (33)$$

According to Eqs. (14) and (12), Eq. (33) results in

$$\mathbf{Q}^{\text{inc}(k)} = \boldsymbol{\mu}^{k-1}\left(\mathbb{C}^{\star}\boldsymbol{\mu}^{N}\left(\mathbb{C}\mathbf{Q}^{\text{inc}} + \mathbb{F}\right) + \mathbb{F}^{\star}\right) \qquad k = 1, \ldots, N+1. \quad (34)$$

Considering Eqs. (10) and (5) yields $\mathbf{Q}^{\text{inc}} = \mathbf{Q}^{\text{inc}(N+1)} = \boldsymbol{\mu}^{N-(k-1)}\mathbf{Q}^{\text{inc}(k)}$. As a result, Eq. (34) can be written as

$$\mathbf{Q}^{\text{inc}(k)} = \mathbf{A}_k\mathbf{Q}^{\text{inc}(k)} + \mathbf{B}_k \qquad k = 1, \ldots, N+1, \quad (35)$$

17

where

$$\mathbf{A}_k = \boldsymbol{\mu}^{k-1} \mathbb{C}^{\star} \boldsymbol{\mu}^N \mathbb{C} \boldsymbol{\mu}^{N-(k-1)} \qquad k = 1, \ldots, N+1, \tag{36}$$

$$\mathbf{B}_k = \boldsymbol{\mu}^{k-1} \left(\mathbb{C}^{\star} \boldsymbol{\mu}^N \mathbb{F} + \mathbb{F}^{\star} \right) \qquad k = 1, \ldots, N+1. \tag{37}$$

Here, $\mathbf{A}_k$ is a $n \times n$ matrix that denotes the attenuation of wave amplitudes induced by two reflections (one for each boundary) after one forward and backward passing of waves along the waveguide, i.e. until the waves reach the starting position at the substructure k. Otherwise, $\mathbf{B}_k$ is a $n \times 1$ vector that denotes the influence of excitation sources during such a forward and backward passing of waves along the waveguide. Expressing Eq. (35) by recurrence, after $s - 1$ iterations, leads to

$$(\mathbf{I}_n - \mathbf{A}_k^s) \mathbf{Q}^{\texttt{inc}(k)} = \mathbf{E}_s^{(k)} \qquad k = 1, \ldots, N+1 \quad \forall s \geq 1, \tag{38}$$

where $\mathbf{E}_s^{(k)}$ represents the vector of wave amplitudes resulting from s forward and backward passings of waves along the waveguide:

$$\mathbf{E}_s^{(k)} = \left(\sum_{p=0}^{s-1} \mathbf{A}_k^p \right) \mathbf{B}_k \qquad k = 1, \ldots, N+1 \quad \forall s \geq 1. \tag{39}$$

On the other hand, considering a reduced wave basis $\{\widetilde{\boldsymbol{\Phi}}_j\}_j$ (i.e. with a same number $m \leq n$ of incident and reflected wave modes) instead of the full wave basis $\{\boldsymbol{\Phi}_j\}_j$, the vector of wave amplitudes is to be expressed as $\widetilde{\mathbf{Q}}^{\texttt{inc}(k)}$. Considering the aforementioned derivations simply yields

$$(\mathbf{I}_m - \widetilde{\mathbf{A}}_k^s) \widetilde{\mathbf{Q}}^{\texttt{inc}(k)} = \widetilde{\mathbf{E}}_s^{(k)} \qquad k = 1, \ldots, N+1 \quad \forall s \geq 1, \tag{40}$$

where the tilde sign means that vectors and matrices have been expressed using the reduced wave basis $\{\widetilde{\boldsymbol{\Phi}}_j\}_j$ instead of the full wave basis $\{\boldsymbol{\Phi}_j\}_j$. In this case, $\widetilde{\mathbf{A}}_k$ and $\widetilde{\mathbf{E}}_k$ refer to a $m \times m$ matrix and a $m \times 1$ vector, respectively, whose expressions follow directly from Eqs. (36) and (39).

18

Eqs. (38) and (40) involve the vectors of wave amplitudes $\mathbf{Q}^{\mathrm{inc}(k)}$ and $\widetilde{\mathbf{Q}}^{\mathrm{inc}(k)}$, respectively. They can be simplified provided that the following assumption is made:

Assumption 1. *The spectral radii of the matrices* $\mathbf{A}_k$ *and* $\widetilde{\mathbf{A}}_k$ *are less than one, i.e.* $\rho(\mathbf{A}_k) < 1$ *and* $\rho(\widetilde{\mathbf{A}}_k) < 1$.

This assumption can be justified as follows. From Eq. (36), since $\rho(\mathbf{A}_k) \leq ||\mathbf{A}_k||$ and $\rho(\widetilde{\mathbf{A}}_k) \leq ||\widetilde{\mathbf{A}}_k||$ (by definition of the spectral radius), it is easy to see that $\rho(\mathbf{A}_k) \leq ||\boldsymbol{\mu}||^{2N} ||\mathbb{C}|| \, ||\mathbb{C}^{\star}||$ while $\rho(\widetilde{\mathbf{A}}_k) \leq ||\widetilde{\boldsymbol{\mu}}||^{2N} ||\widetilde{\mathbb{C}}|| \, ||\widetilde{\mathbb{C}}^{\star}||$ (N being the number of substructures considered along the waveguide). Since $||\widetilde{\boldsymbol{\mu}}|| \leq ||\boldsymbol{\mu}|| < 1$ (see below Eq. (20)), Assumption 1 appears to be satisfied provided that (i) $||\boldsymbol{\mu}||$ is small enough compared to one (this in fact depends on the waveguide damping [15]) and (ii) a sufficient number N of substructures is considered, i.e. the waveguide is long enough.

Assumption 1 particularly means that there exists an integer $s_0 \geq 1$ such that $||\mathbf{A}_k^s|| < 1$ and $||\widetilde{\mathbf{A}}_k^s|| < 1 \; \forall s \geq s_0$. In this framework, invoking Neumann series expansions $(\mathbf{I}_n - \mathbf{A}_k^s)^{-1} = \mathbf{I}_n + \sum_{q=1}^{\infty} \mathbf{A}_k^{sq}$ and $(\mathbf{I}_m - \widetilde{\mathbf{A}}_k^s)^{-1} = \mathbf{I}_m + \sum_{q=1}^{\infty} \widetilde{\mathbf{A}}_k^{sq}$ in Eqs. (38) and (40) enables the vectors of wave amplitudes $\mathbf{Q}^{\mathrm{inc}(k)}$ and $\widetilde{\mathbf{Q}}^{\mathrm{inc}(k)}$ to be expressed as

$$\mathbf{Q}^{\mathrm{inc}(k)} = \mathbf{E}_s^{(k)} + \left(\sum_{q=1}^{\infty} \mathbf{A}_k^{sq} \right) \mathbf{E}_s^{(k)} \qquad k = 1, \ldots, N+1 \quad \forall s \geq s_0, \tag{41}$$

and

$$\widetilde{\mathbf{Q}}^{\mathrm{inc}(k)} = \widetilde{\mathbf{E}}_s^{(k)} + \left(\sum_{q=1}^{\infty} \widetilde{\mathbf{A}}_k^{sq} \right) \widetilde{\mathbf{E}}_s^{(k)} \qquad k = 1, \ldots, N+1 \quad \forall s \geq s_0. \tag{42}$$

19

The convergence of the Neumann series involved in these equations is readily proved since $||\mathbf{A}_k^s|| < 1$ and $||\widetilde{\mathbf{A}}_k^s|| < 1$. In these equations, $\mathbf{E}_s^{(k)}$ and $\widetilde{\mathbf{E}}_s^{(k)}$ denote the contributions of s forward and backward passings of waves along the waveguide for describing the vectors of wave amplitudes $\mathbf{Q}^{\text{inc}(k)}$ and $\widetilde{\mathbf{Q}}^{\text{inc}(k)}$ (see above); on the other hand, $(\sum_{q=1}^{\infty} \mathbf{A}_k^{sq})\mathbf{E}_s^{(k)}$ and $(\sum_{q=1}^{\infty} \widetilde{\mathbf{A}}_k^{sq})\widetilde{\mathbf{E}}_s^{(k)}$ result from the consideration of additional sets of s forward and backward wave passings for describing these vectors of wave amplitudes.

3.3. Error norms

3.3.1. General expressions

It is worth recalling that the error norm $||\Delta\mathbf{Q}^{\text{inc}(k)}||$ is estimated from Eq. (32) by means of the error norms $||\widetilde{\mathbf{Q}}^{\text{inc}(k)} - \widetilde{\mathcal{L}}\mathbf{Q}^{\text{inc}(k)}||$ and $||\mathcal{L}_{\mathbf{r}}\mathbf{Q}^{\text{inc}(k)}||$. In Appendices A and B, it is shown that these error norms are bounded as

$$
\begin{aligned}
&||\widetilde{\mathbf{Q}}^{\text{inc}(k)} - \widetilde{\mathcal{L}}\mathbf{Q}^{\text{inc}(k)}|| \\
&\leq \left(\sum_{q=0}^{\infty} ||\widetilde{\mathbf{A}}_k^s||^q \right) ||\widetilde{\mathbf{E}}_s^{(k)} - \widetilde{\mathcal{L}}\mathbf{E}_s^{(k)}|| + \left(\sum_{q=1}^{\infty} ||\widetilde{\mathbf{A}}_k^{sq}\widetilde{\mathcal{L}} - \widetilde{\mathcal{L}}\mathbf{A}_k^{sq}|| \right) ||\mathbf{E}_s^{(k)}|| \\
&\hspace{6cm} k = 1, \ldots, N+1 \quad \forall s \geq s_0, \quad (43)
\end{aligned}
$$

and

$$
||\mathcal{L}_{\mathbf{r}}\mathbf{Q}^{\text{inc}(k)}|| \leq \left(\sum_{q=0}^{\infty} ||\mathbf{A}_k^s||^q \right) ||\mathcal{L}_{\mathbf{r}}\mathbf{E}_s^{(k)}|| + \left(\sum_{q=1}^{\infty} ||\mathcal{L}_{\mathbf{r}}\mathbf{A}_k^{sq}\widetilde{\mathcal{L}}^T|| \right) ||\mathbf{E}_s^{(k)}||
$$

$$
k = 1, \ldots, N+1 \quad \forall s \geq s_0. \quad (44)
$$

Remarks.

- *Bound of $||\widetilde{\mathbf{Q}}^{\text{inc}(k)} - \widetilde{\mathcal{L}}\mathbf{Q}^{\text{inc}(k)}||$ (Eq. (43)):*
  Since $||\widetilde{\mathbf{A}}_k^s|| < 1$ for $s \geq s_0$ (cf. Section 3.2), it turns out that $\sum_{q=0}^{\infty} ||\widetilde{\mathbf{A}}_k^s||^q =$

$1/(1-||\widetilde{\mathbf{A}}_k^s||)$ (this is a classical result of geometric series). Thus, apart from the consideration of the matrix norm $||\widetilde{\mathbf{A}}_k^s||$, the first term on the right hand side of Eq. (43) turns out to be linked with the error induced for approximating $\widetilde{\mathcal{L}}\mathbf{E}_s^{(k)}$ by $\widetilde{\mathbf{E}}_s^{(k)}$, i.e. by means of the reduced wave basis $\{\widetilde{\boldsymbol{\Phi}}_j\}_j$. The second term is more complicated to understand. It actually represents the error induced for approximating a set of $m \times n$ matrices $\{\widetilde{\mathcal{L}}\mathbf{A}_k^{sq}\}_q$ by means of $m \times n$ matrices $\{\widetilde{\mathbf{A}}_k^{sq}\widetilde{\mathcal{L}}\}_q$ derived from the reduced wave basis $\{\widetilde{\boldsymbol{\Phi}}_j\}_j$. If one supposes that $\widetilde{\mathcal{L}} = [\mathbf{I}_m|\mathbf{0}_{m\times(n-m)}]$ and $\mathcal{L}_{\mathbf{r}} = [\mathbf{0}_{(n-m)\times m}|\mathbf{I}_{n-m}]$ yields $\widetilde{\mathcal{L}}\mathbf{A}_k^{sq} = [\widetilde{\mathcal{L}}\mathbf{A}_k^{sq}\widetilde{\mathcal{L}}^T|\widetilde{\mathcal{L}}\mathbf{A}_k^{sq}\mathcal{L}_{\mathbf{r}}^T]$ and $\widetilde{\mathbf{A}}_k^{sq}\widetilde{\mathcal{L}} = [\widetilde{\mathbf{A}}_k^{sq}|\mathbf{0}_{m\times(n-m)}]$: thus, the issue is to approximate $\{\widetilde{\mathcal{L}}\mathbf{A}_k^{sq}\widetilde{\mathcal{L}}^T\}_q$ by means of $\{\widetilde{\mathbf{A}}_k^{sq}\}_q$, but also to reduce the norms of a set of coupling matrices $\{\widetilde{\mathcal{L}}\mathbf{A}_k^{sq}\mathcal{L}_{\mathbf{r}}^T\}_q$.

- *Bound of $||\mathcal{L}_{\mathbf{r}}\mathbf{Q}^{\mathtt{inc}(k)}||$ (Eq. (44)):*

  Since $||\mathbf{A}_k^s|| < 1$ for $s \geq s_0$ (cf. Section 3.2), it turns out that $\sum_{q=0}^{\infty}||\mathbf{A}_k^s||^q = 1/(1-||\mathbf{A}_k^s||)$. Thus, apart from the consideration of the matrix norm $||\mathbf{A}_k^s||$, the first term on the right hand side of Eq. (44) turns out to be linked with the error induced when the vector $\mathcal{L}_{\mathbf{r}}\mathbf{E}_s^{(k)}$ is neglected for describing $\mathbf{Q}^{\mathtt{inc}(k)}$, i.e. when the residual wave modes are omitted. Otherwise, the second term relates the error induced when a set of coupling matrices $\{\mathcal{L}_{\mathbf{r}}\mathbf{A}_k^{sq}\widetilde{\mathcal{L}}^T\}_q$ are neglected for expressing $\mathbf{Q}^{\mathtt{inc}(k)}$.

A bound of $||\Delta\mathbf{Q}^{\mathtt{inc}(k)}||$ is obtained by summing Eqs. (43) and (44). It is worth noting that this bound is to be addressed for every substructure boundary k ($k = 1,\ldots,N+1$) considered along the waveguide (cf. Figure 2). To avoid the issue of analyzing those $N+1$ values of the bound, it is proposed to treat with its maximum value only. Considering that Eqs. (43) and (44) are expressed in terms of $\mathbf{E}_s^{(k)}$ and $\widetilde{\mathbf{E}}_s^{(k)}$, i.e. by means of $\mathbf{B}_k$ and $\widetilde{\mathbf{B}}_k$ (cf. Eq. (39)), the maximum bound of

$||\Delta\mathbf{Q}^{\mathtt{inc}(k)}||$ is likely to be reached at the substructure boundary where the norms $||\mathbf{B}_k||$ and $||\widetilde{\mathbf{B}}_k||$ are maximum. This substructure boundary is easily found to be the left end of the waveguide – namely the substructure boundary 1 – where $\mathbf{B}_1 = \mathbb{C}^\star\boldsymbol{\mu}^N\mathbb{F} + \mathbb{F}^\star$. The fact that $||\mathbf{B}_k||$ and $||\widetilde{\mathbf{B}}_k||$ are maximum at this location is readily proved from Eq. (37), considering that $||\mathbf{B}_k|| \leq ||\boldsymbol{\mu}||^{k-1}||\mathbf{B}_1|| < ||\mathbf{B}_1||$ and $||\widetilde{\mathbf{B}}_k|| \leq ||\widetilde{\boldsymbol{\mu}}||^{k-1}||\widetilde{\mathbf{B}}_1|| < ||\widetilde{\mathbf{B}}_1||$ (because $||\boldsymbol{\mu}|| < 1$ and $||\widetilde{\boldsymbol{\mu}}|| < 1$). Considering this substructure boundary 1, the vector of wave amplitudes $\mathbf{Q}^{\mathtt{inc}(1)}$ is to be expressed as $\mathbf{Q}^{\mathtt{ref}\star}$ (see Section 2.2), while the vector $\mathbf{E}_s^{(1)}$ can be expressed as

$$\mathbf{E}_s = \left(\sum_{p=0}^{s-1}\mathbf{A}^p\right)\mathbf{B} \qquad \forall s \geq 1, \tag{45}$$

where

$$\mathbf{A} = \mathbf{A}_1 = \mathbb{C}^\star\boldsymbol{\mu}^N\mathbb{C}\boldsymbol{\mu}^N \quad , \quad \mathbf{B} = \mathbf{B}_1 = \mathbb{C}^\star\boldsymbol{\mu}^N\mathbb{F} + \mathbb{F}^\star. \tag{46}$$

To summarize, a bound of $||\Delta\mathbf{Q}^{\mathtt{inc}(k)}||$ follows as $||\Delta\mathbf{Q}^{\mathtt{inc}(k)}|| \leq ||\Delta\mathbf{Q}^{\mathtt{ref}\star}||\ \forall k$, where $||\Delta\mathbf{Q}^{\mathtt{ref}\star}||$ is bounded from Eqs. (32), (43) and (44) as

$$\begin{aligned}
&||\Delta\mathbf{Q}^{\mathtt{ref}\star}|| \\
&\leq \left(\sum_{q=0}^{\infty}||\widetilde{\mathbf{A}}^s||^q\right)||\widetilde{\mathbf{E}}_s - \widetilde{\mathcal{L}}\mathbf{E}_s|| + \left(\sum_{q=0}^{\infty}||\mathbf{A}^s||^q\right)||\mathcal{L}_\mathtt{r}\mathbf{E}_s|| \\
&\quad + \left(\sum_{q=1}^{\infty}||\widetilde{\mathbf{A}}^{sq}\widetilde{\mathcal{L}} - \widetilde{\mathcal{L}}\mathbf{A}^{sq}||\right)||\mathbf{E}_s|| + \left(\sum_{q=1}^{\infty}||\mathcal{L}_\mathtt{r}\mathbf{A}^{sq}\widetilde{\mathcal{L}}^T||\right)||\mathbf{E}_s|| \\
&\hspace{10cm} \forall s \geq s_0. \tag{47}
\end{aligned}$$

On the other hand, a bound of $||\Delta\mathbf{Q}^{\mathtt{ref}(k)}||$ (i.e. invoking the amplitudes of the reflected wave modes) is deduced from the summation of Eqs. (43) and (44), considering the following substitutions: $\mathbf{A}_k \rightarrow \mathbf{A}_k^\star = \boldsymbol{\mu}^{N-(k-1)}\mathbb{C}\boldsymbol{\mu}^N\mathbb{C}^\star\boldsymbol{\mu}^{k-1}$

and $\mathbf{B}_k \to \mathbf{B}_k^\star = \boldsymbol{\mu}^{N-(k-1)}(\mathbb{C}\boldsymbol{\mu}^N\mathbb{F}^\star + \mathbb{F})$ (such expressions of $\mathbf{A}_k^\star$ and $\mathbf{B}_k^\star$ are obtained by expressing $\mathbf{Q}^{\mathtt{ref}(k)}$ on the same scheme as $\mathbf{Q}^{\mathtt{inc}(k)}$ (cf. Section 3.2), i.e. considering Eqs. (9), (11-14)). Also, the bound of $||\Delta\mathbf{Q}^{\mathtt{ref}(k)}||$ follows from the consideration of the maximum values of $||\mathbf{B}_k^\star||$ and $||\widetilde{\mathbf{B}}_k^\star||$: in this case, the corresponding substructure boundary is found to be the right end of the waveguide – namely the substructure boundary $N+1$ – where

$$\mathbf{A}^\star = \mathbf{A}_{N+1}^\star = \mathbb{C}\boldsymbol{\mu}^N\mathbb{C}^\star\boldsymbol{\mu}^N \quad , \quad \mathbf{B}^\star = \mathbf{B}_{N+1}^\star = \mathbb{C}\boldsymbol{\mu}^N\mathbb{F}^\star + \mathbb{F}. \tag{48}$$

To summarize, a bound of $||\Delta\mathbf{Q}^{\mathtt{ref}(k)}||$ follows as $||\Delta\mathbf{Q}^{\mathtt{ref}(k)}|| \le ||\Delta\mathbf{Q}^{\mathtt{ref}}|| \ \forall k$, where $||\Delta\mathbf{Q}^{\mathtt{ref}}||$ is bounded as

$$\begin{aligned}
||\Delta\mathbf{Q}^{\mathtt{ref}}|| \\
\le \left(\sum_{q=0}^\infty ||\widetilde{\mathbf{A}}^{\star s}||^q\right) ||\widetilde{\mathbf{E}}_s^\star - \widetilde{\mathcal{L}}\mathbf{E}_s^\star|| + \left(\sum_{q=0}^\infty ||\mathbf{A}^{\star s}||^q\right) ||\mathcal{L}_{\mathtt{r}}\mathbf{E}_s^\star|| \\
+ \left(\sum_{q=1}^\infty ||\widetilde{\mathbf{A}}^{\star sq}\widetilde{\mathcal{L}} - \widetilde{\mathcal{L}}\mathbf{A}^{\star sq}||\right) ||\mathbf{E}_s^\star|| + \left(\sum_{q=1}^\infty ||\mathcal{L}_{\mathtt{r}}\mathbf{A}^{\star sq}\widetilde{\mathcal{L}}^T||\right) ||\mathbf{E}_s^\star|| \\
\forall s \ge s_0^\star, \tag{49}
\end{aligned}$$

where

$$\mathbf{E}_s^\star = \left(\sum_{p=0}^{s-1}\mathbf{A}^{\star p}\right)\mathbf{B}^\star \qquad \forall s \ge 1. \tag{50}$$

In Eq. (49), $s_0^\star \ge 1$ is an integer defined such that $||\mathbf{A}_k^{\star s}|| < 1$ and $||\widetilde{\mathbf{A}}_k^{\star s}|| < 1$ for $s \ge s_0^\star$. To ensure the existence of such an integer, it is assumed that the spectral radii of the matrices $\mathbf{A}_k^\star$ and $\widetilde{\mathbf{A}}_k^\star$ are less than one, i.e. as already stated for the matrices $\mathbf{A}_k$ and $\widetilde{\mathbf{A}}_k$ (see Assumption 1).

23

3.3.2. Simplified expressions

According to Eqs. (26) and (27), the key issue behind the proposed MOR strategy is to minimize the term $||\Delta \mathbf{Q}^{\mathtt{inc}(k)}|| + ||\Delta \mathbf{Q}^{\mathtt{ref}(k)}||$. A bound for this term is found by summing Eqs. (47) and (49). At first glance, the minimization of the resulting expression appears quite complex to carry out with regard to the different summations which are involved in these equations. To solve this issue, further simplifications are proposed. Eq. (47) is considered first.

The first idea behind the simplification of Eq. (47) is to introduce the following relative errors $\epsilon_1^{\mathbf{E}}$, $\epsilon_2^{\mathbf{E}}$, $\epsilon_1^{\mathbf{A}}$ and $\epsilon_2^{\mathbf{A}}$:

$$\epsilon_1^{\mathbf{E}} = \frac{||\widetilde{\mathbf{E}}_s - \widetilde{\mathcal{L}}\mathbf{E}_s||}{||\mathbf{E}_s||} \quad , \quad \epsilon_2^{\mathbf{E}} = \frac{||\mathcal{L}_{\mathtt{r}}\mathbf{E}_s||}{||\mathbf{E}_s||}, \tag{51}$$

$$\epsilon_1^{\mathbf{A}} = \frac{||\widetilde{\mathbf{A}}^s\widetilde{\mathcal{L}} - \widetilde{\mathcal{L}}\mathbf{A}^s||}{||\mathbf{A}^s||} \quad , \quad \epsilon_2^{\mathbf{A}} = \frac{||\mathcal{L}_{\mathtt{r}}\mathbf{A}^s\widetilde{\mathcal{L}}^T||}{||\mathbf{A}^s||}. \tag{52}$$

Also, it is proposed to consider the following assumption:

Assumption 2. *The norms of the matrices* $\mathbf{A}^s$ *and* $\widetilde{\mathbf{A}}^s$ *are such that* $||\widetilde{\mathbf{A}}^s|| \leq ||\mathbf{A}^s||$.

This assumption appears to be satisfied provided that the relative error $\epsilon_1^{\mathbf{A}}$ is small enough [1], which is what is expected for minimizing $||\Delta \mathbf{Q}^{\mathtt{inc}(k)}||$ (see later). In other words, this assumption does not seem to constitute a penalization of the minimization procedure.

---

[1]In this case, one has $\widetilde{\mathbf{A}}^s\widetilde{\mathcal{L}} \approx \widetilde{\mathcal{L}}\mathbf{A}^s$, i.e. $||\widetilde{\mathbf{A}}^s\widetilde{\mathcal{L}}|| \approx ||\widetilde{\mathcal{L}}\mathbf{A}^s||$ and thus $||\widetilde{\mathbf{A}}^s|| \leq ||\mathbf{A}^s||$, because $||\widetilde{\mathbf{A}}^s\widetilde{\mathcal{L}}|| = ||\widetilde{\mathbf{A}}^s||$ (indeed, $\widetilde{\mathbf{A}}^s\widetilde{\mathcal{L}}$ can be written as $\left[\widetilde{\mathbf{A}}^s|\mathbf{0}_{m\times(n-m)}\right]$ (see Remarks below Eq. (44))) while $||\widetilde{\mathcal{L}}\mathbf{A}^s|| \leq ||\widetilde{\mathcal{L}}||\,||\mathbf{A}^s|| = ||\mathbf{A}^s||$ since $||\widetilde{\mathcal{L}}|| = 1$ (see below Eq. (B-2)).

The second idea behind the simplification of Eq. (47) lies in the following proposition:

Proposition 2. $||\widetilde{\mathbf{A}}^{sq}\widetilde{\mathcal{L}} - \widetilde{\mathcal{L}}\mathbf{A}^{sq}||$ and $||\mathcal{L}_{\mathbf{r}}\mathbf{A}^{sq}\widetilde{\mathcal{L}}^{T}||$ are bounded as

$$||\widetilde{\mathbf{A}}^{sq}\widetilde{\mathcal{L}} - \widetilde{\mathcal{L}}\mathbf{A}^{sq}|| \leq q\epsilon_1^{\mathbf{A}}||\mathbf{A}^s||^q \quad , \quad ||\mathcal{L}_{\mathbf{r}}\mathbf{A}^{sq}\widetilde{\mathcal{L}}^{T}|| \leq q\epsilon_2^{\mathbf{A}}||\mathbf{A}^s||^q \qquad \forall q \geq 1.$$
(53)

Proof. To prove that $||\widetilde{\mathbf{A}}^{sq}\widetilde{\mathcal{L}} - \widetilde{\mathcal{L}}\mathbf{A}^{sq}|| \leq q\epsilon_1^{\mathbf{A}}||\mathbf{A}^s||^q$, let us consider the decompositions $\widetilde{\mathbf{A}}^{sq}\widetilde{\mathcal{L}} = \widetilde{\mathbf{A}}^s\widetilde{\mathbf{A}}^{s(q-1)}\widetilde{\mathcal{L}}$ and $\widetilde{\mathcal{L}}\mathbf{A}^{sq} = \widetilde{\mathcal{L}}\mathbf{A}^s\mathbf{A}^{s(q-1)}$. Considering that $\widetilde{\mathcal{L}}\mathbf{A}^s = \widetilde{\mathcal{L}}\mathbf{A}^s - \widetilde{\mathbf{A}}^s\widetilde{\mathcal{L}} + \widetilde{\mathbf{A}}^s\widetilde{\mathcal{L}}$ yields

$$\widetilde{\mathbf{A}}^{sq}\widetilde{\mathcal{L}} - \widetilde{\mathcal{L}}\mathbf{A}^{sq} = \widetilde{\mathbf{A}}^s(\widetilde{\mathbf{A}}^{s(q-1)}\widetilde{\mathcal{L}} - \widetilde{\mathcal{L}}\mathbf{A}^{s(q-1)}) + (\widetilde{\mathbf{A}}^s\widetilde{\mathcal{L}} - \widetilde{\mathcal{L}}\mathbf{A}^s)\mathbf{A}^{s(q-1)} \qquad \forall q \geq 1.$$
(54)

Introducing the notations $\Delta_q = \widetilde{\mathbf{A}}^{sq}\widetilde{\mathcal{L}} - \widetilde{\mathcal{L}}\mathbf{A}^{sq}$, Eq. (54) reduces to $\Delta_q = \widetilde{\mathbf{A}}^s\Delta_{q-1} + \Delta_1\mathbf{A}^{s(q-1)}$. This defines a recurrence equation that can be solved without difficulty to yield $\Delta_q = \sum_{t=1}^{q} \widetilde{\mathbf{A}}^{s(t-1)}\Delta_1\mathbf{A}^{s(q-t)}$. Considering that $||\widetilde{\mathbf{A}}^{s(t-1)}|| \leq ||\widetilde{\mathbf{A}}^s||^{t-1}$ and $||\mathbf{A}^{s(q-t)}|| \leq ||\mathbf{A}^s||^{q-t}$ leads to $||\Delta_q|| \leq \sum_{t=1}^{q} ||\widetilde{\mathbf{A}}^s||^{t-1}||\mathbf{A}^s||^{q-t}||\Delta_1||$. Taking into account that $||\widetilde{\mathbf{A}}^s|| \leq ||\mathbf{A}^s||$ (Assumption 2) yields $||\Delta_q|| \leq \sum_{t=1}^{q} ||\Delta_1|| \, ||\mathbf{A}^s||^{q-1} = q||\Delta_1|| \, ||\mathbf{A}^s||^{q-1}$. The expected result is found by means of Eq. (52) since $||\Delta_1|| = \epsilon_1^{\mathbf{A}}||\mathbf{A}^s||$.

To prove that $||\mathcal{L}_{\mathbf{r}}\mathbf{A}^{sq}\widetilde{\mathcal{L}}^{T}|| \leq q\epsilon_2^{\mathbf{A}}||\mathbf{A}^s||$, let us consider the decomposition $\mathcal{L}_{\mathbf{r}}\mathbf{A}^{sq}\widetilde{\mathcal{L}}^{T} = \mathcal{L}_{\mathbf{r}}\mathbf{A}^{s(q-1)}\mathbf{A}^s\widetilde{\mathcal{L}}^{T}$. Since $\widetilde{\mathcal{L}}^{T}\widetilde{\mathcal{L}} + \mathcal{L}_{\mathbf{r}}^{T}\mathcal{L}_{\mathbf{r}} = \mathbf{I}_n$ (cf. above Proposition 1), it follows that $\mathcal{L}_{\mathbf{r}}\mathbf{A}^{sq}\widetilde{\mathcal{L}}^{T} = \mathcal{L}_{\mathbf{r}}\mathbf{A}^{s(q-1)}\widetilde{\mathcal{L}}^{T}\widetilde{\mathcal{L}}\mathbf{A}^s\widetilde{\mathcal{L}}^{T} + \mathcal{L}_{\mathbf{r}}\mathbf{A}^{s(q-1)}\mathcal{L}_{\mathbf{r}}^{T}\mathcal{L}_{\mathbf{r}}\mathbf{A}^s\widetilde{\mathcal{L}}^{T}$. Considering that $||\widetilde{\mathcal{L}}\mathbf{A}^s\widetilde{\mathcal{L}}^{T}|| \leq ||\mathbf{A}^s||$ and $||\mathcal{L}_{\mathbf{r}}\mathbf{A}^{s(q-1)}\mathcal{L}_{\mathbf{r}}^{T}|| \leq ||\mathbf{A}^{s(q-1)}||$ (since $||\widetilde{\mathcal{L}}^{T}|| = ||\mathcal{L}_{\mathbf{r}}^{T}|| = ||\widetilde{\mathcal{L}}|| = ||\mathcal{L}_{\mathbf{r}}|| = 1$ (see below Eq. (B-2))) while $||\mathbf{A}^{s(q-1)}|| \leq ||\mathbf{A}^s||^{q-1}$

yields $||\mathcal{L}_{\mathbf{r}}\mathbf{A}^{sq}\widetilde{\mathcal{L}}^{T}|| \leq ||\mathcal{L}_{\mathbf{r}}\mathbf{A}^{s(q-1)}\widetilde{\mathcal{L}}^{T}||\,||\mathbf{A}^{s}|| + ||\mathbf{A}^{s}||^{q-1}||\mathcal{L}_{\mathbf{r}}\mathbf{A}^{s}\widetilde{\mathcal{L}}^{T}||$. This defines a recurrence relation whose solution is $||\mathcal{L}_{\mathbf{r}}\mathbf{A}^{sq}\widetilde{\mathcal{L}}^{T}|| \leq \sum_{t=1}^{q}||\mathbf{A}^{s}||^{t-1}||\mathcal{L}_{\mathbf{r}}\mathbf{A}^{s}\widetilde{\mathcal{L}}^{T}||\,||\mathbf{A}^{s}||^{q-t}$. This yields $||\mathcal{L}_{\mathbf{r}}\mathbf{A}^{sq}\widetilde{\mathcal{L}}^{T}|| \leq q||\mathcal{L}_{\mathbf{r}}\mathbf{A}^{s}\widetilde{\mathcal{L}}^{T}||\,||\mathbf{A}^{s}||^{q-1}$. The expected result is found by means of Eq. (52) since $||\mathcal{L}_{\mathbf{r}}\mathbf{A}^{s}\widetilde{\mathcal{L}}^{T}|| = \epsilon_{2}^{\mathbf{A}}||\mathbf{A}^{s}||$. $\quad\square$

According to Assumption 2 and Proposition 2, Eqs. (51), (52) and (53) enable Eq. (47) to be expressed as

$$||\Delta\mathbf{Q}^{\mathtt{ref}\star}|| \leq \left[\left(\sum_{q=0}^{\infty}||\mathbf{A}^{s}||^{q}\right)(\epsilon_{1}^{\mathbf{E}} + \epsilon_{2}^{\mathbf{E}}) + \left(\sum_{q=1}^{\infty}q||\mathbf{A}^{s}||^{q}\right)(\epsilon_{1}^{\mathbf{A}} + \epsilon_{2}^{\mathbf{A}})\right]||\mathbf{E}_{s}||$$
$$\forall s \geq s_{0}. \quad (55)$$

Further simplifications of this equation can be brought taking into account some classical results of the theory of mathematical series, for $||\mathbf{A}^{s}|| < 1$:

$$\sum_{q=0}^{\infty}||\mathbf{A}^{s}||^{q} = \lim_{u\to\infty}\left(\frac{1 - ||\mathbf{A}^{s}||^{u+1}}{1 - ||\mathbf{A}^{s}||}\right) = \frac{1}{1 - ||\mathbf{A}^{s}||} \qquad \forall s \geq s_{0}, \quad (56)$$

$$\sum_{q=1}^{\infty}q||\mathbf{A}^{s}||^{q} = \lim_{u\to\infty}\left(||\mathbf{A}^{s}||\frac{1 - (u+1)||\mathbf{A}^{s}||^{u} + u||\mathbf{A}^{s}||^{u+1}}{(1 - ||\mathbf{A}^{s}||)^{2}}\right)$$
$$= \frac{||\mathbf{A}^{s}||}{(1 - ||\mathbf{A}^{s}||)^{2}} \qquad \forall s \geq s_{0}, \quad (57)$$

where the integer s_{0} is defined such that $||\mathbf{A}^{s}|| < 1 \ \forall s \geq s_{0}$ (see above Eq. (41)). The result provided by Eq. (56) is classical while Eq. (57) follows from the consideration that $\sum_{q=1}^{u}q||\mathbf{A}^{s}||^{q} = ||\mathbf{A}^{s}||\partial(\sum_{q=0}^{u}||\mathbf{A}^{s}||^{q})/\partial||\mathbf{A}^{s}||$. Considering Eqs. (56) and (57) yields Eq. (55) to be written as

$$||\Delta\mathbf{Q}^{\mathtt{ref}\star}|| \leq \left[(\epsilon_{1}^{\mathbf{E}} + \epsilon_{2}^{\mathbf{E}}) + \frac{||\mathbf{A}^{s}||}{1 - ||\mathbf{A}^{s}||}(\epsilon_{1}^{\mathbf{A}} + \epsilon_{2}^{\mathbf{A}})\right]\frac{||\mathbf{E}_{s}||}{1 - ||\mathbf{A}^{s}||}$$
$$\forall s \geq s_{0}. \quad (58)$$

26

Otherwise, Eq. (38) yields $\mathbf{E}_s = (\mathbf{I}_n - \mathbf{A}^s)\mathbf{Q}^{\texttt{inc}(1)} = (\mathbf{I}_n - \mathbf{A}^s)\mathbf{Q}^{\texttt{ref}\star}$, i.e. $||\mathbf{E}_s|| \leq (1 + ||\mathbf{A}^s||)||\mathbf{Q}^{\texttt{ref}\star}||$. As a result, Eq. (58) leads to

$$||\Delta\mathbf{Q}^{\texttt{ref}\star}|| \leq \left[(\epsilon_1^{\mathbf{E}} + \epsilon_2^{\mathbf{E}}) + \frac{||\mathbf{A}^s||}{1 - ||\mathbf{A}^s||}(\epsilon_1^{\mathbf{A}} + \epsilon_2^{\mathbf{A}}) \right] \frac{1 + ||\mathbf{A}^s||}{1 - ||\mathbf{A}^s||}||\mathbf{Q}^{\texttt{ref}\star}||$$
$$\forall s \geq s_0. \quad (59)$$

Eq. (59) provides a simplified bound of the error norm $||\Delta\mathbf{Q}^{\texttt{inc}(k)}||$, $\forall k$ (cf. above Eq. (47)). On the other hand, a bound of the error norm $||\Delta\mathbf{Q}^{\texttt{ref}(k)}||$ (cf. above Eq. (49)) follows from Eq. (59), considering the conventions $\mathbf{A} \rightarrow \mathbf{A}^\star$, $\mathbf{B} \rightarrow \mathbf{B}^\star$ and provided that $||\widetilde{\mathbf{A}}^{\star s}|| \leq ||\mathbf{A}^{\star s}||$ (cf. Assumption 2). This bound is readily written as

$$||\Delta\mathbf{Q}^{\texttt{ref}}|| \leq \left[(\epsilon_1^{\mathbf{E}^\star} + \epsilon_2^{\mathbf{E}^\star}) + \frac{||\mathbf{A}^{\star s}||}{1 - ||\mathbf{A}^{\star s}||}(\epsilon_1^{\mathbf{A}^\star} + \epsilon_2^{\mathbf{A}^\star}) \right] \frac{1 + ||\mathbf{A}^{\star s}||}{1 - ||\mathbf{A}^{\star s}||}||\mathbf{Q}^{\texttt{ref}}||$$
$$\forall s \geq s_0^\star. \quad (60)$$

Thus, considering Eqs. (59) and (60), a bound of $||\Delta\mathbf{Q}^{\texttt{inc}(k)}|| + ||\Delta\mathbf{Q}^{\texttt{ref}(k)}||$ results in

$$||\Delta\mathbf{Q}^{\texttt{ref}\star}|| + ||\Delta\mathbf{Q}^{\texttt{ref}}||$$
$$\leq \left[(\epsilon_1^{\mathbf{E}} + \epsilon_2^{\mathbf{E}}) + \frac{||\mathbf{A}^s||}{1 - ||\mathbf{A}^s||}(\epsilon_1^{\mathbf{A}} + \epsilon_2^{\mathbf{A}}) \right] \frac{1 + ||\mathbf{A}^s||}{1 - ||\mathbf{A}^s||}||\mathbf{Q}^{\texttt{ref}\star}||$$
$$+ \left[(\epsilon_1^{\mathbf{E}^\star} + \epsilon_2^{\mathbf{E}^\star}) + \frac{||\mathbf{A}^{\star s}||}{1 - ||\mathbf{A}^{\star s}||}(\epsilon_1^{\mathbf{A}^\star} + \epsilon_2^{\mathbf{A}^\star}) \right] \frac{1 + ||\mathbf{A}^{\star s}||}{1 - ||\mathbf{A}^{\star s}||}||\mathbf{Q}^{\texttt{ref}}||$$
$$\forall s \geq \max\{s_0, s_0^\star\}. \quad (61)$$

Eq. (61) is readily rewritten by means of the following parameter $\mathcal{E}_s$:

$$\mathcal{E}_s = \max \left\{ \left[(\epsilon_1^{\mathbf{E}} + \epsilon_2^{\mathbf{E}}) + \frac{||\mathbf{A}^s||}{1 - ||\mathbf{A}^s||}(\epsilon_1^{\mathbf{A}} + \epsilon_2^{\mathbf{A}}) \right] \frac{1 + ||\mathbf{A}^s||}{1 - ||\mathbf{A}^s||} \right. ,$$
$$\left. \left[(\epsilon_1^{\mathbf{E}^\star} + \epsilon_2^{\mathbf{E}^\star}) + \frac{||\mathbf{A}^{\star s}||}{1 - ||\mathbf{A}^{\star s}||}(\epsilon_1^{\mathbf{A}^\star} + \epsilon_2^{\mathbf{A}^\star}) \right] \frac{1 + ||\mathbf{A}^{\star s}||}{1 - ||\mathbf{A}^{\star s}||} \right\}, \quad (62)$$

which yields

$$||\Delta\mathbf{Q}^{\texttt{ref}\star}|| + ||\Delta\mathbf{Q}^{\texttt{ref}}|| \leq \mathcal{E}_s(||\mathbf{Q}^{\texttt{ref}\star}|| + ||\mathbf{Q}^{\texttt{ref}}||)$$
$$\forall s \geq \max\{s_0, s_0^\star\}. \quad (63)$$

To summarize, according to Eqs. (26) and (27), the error norms $||\widetilde{\mathbf{q}}^{(k)} - \mathbf{q}^{(k)}||$ and $||\widetilde{\mathbf{F}}^{(k)} - \mathbf{F}^{(k)}||$ involved by the reduced WFE matrix formulation for computing the displacements and internal forces (over any substructure boundary k considered along the waveguide) are bounded as

$$||\widetilde{\mathbf{q}}^{(k)} - \mathbf{q}^{(k)}|| \leq \mathcal{E}_s ||\mathbf{\Phi}_{\mathtt{q}}^{\mathtt{inc}}|| (||\mathbf{Q}^{\mathtt{ref}\star}|| + ||\mathbf{Q}^{\mathtt{ref}}||)$$

$$\forall s \geq \mathtt{max}\{s_0, s_0^\star\}, \qquad (64)$$

$$||\widetilde{\mathbf{F}}^{(k)} - \mathbf{F}^{(k)}|| \leq \mathcal{E}_s ||\mathbf{\Phi}_{\mathtt{F}}^{\mathtt{inc}}|| (||\mathbf{Q}^{\mathtt{ref}\star}|| + ||\mathbf{Q}^{\mathtt{ref}}||)$$

$$\forall s \geq \mathtt{max}\{s_0, s_0^\star\}. \qquad (65)$$

In these equations, $||\mathbf{\Phi}_{\mathtt{q}}^{\mathtt{inc}}|| (||\mathbf{Q}^{\mathtt{ref}\star}|| + ||\mathbf{Q}^{\mathtt{ref}}||)$ and $||\mathbf{\Phi}_{\mathtt{F}}^{\mathtt{inc}}|| (||\mathbf{Q}^{\mathtt{ref}\star}|| + ||\mathbf{Q}^{\mathtt{ref}}||)$ can be viewed as bounds of $||\mathbf{q}^{(k)}||$ and $||\mathbf{F}^{(k)}||$ (this is explained since $||\mathbf{Q}^{\mathtt{ref}\star}||$ and $||\mathbf{Q}^{\mathtt{ref}}||$ are expected to be the maximum values of $||\mathbf{Q}^{\mathtt{inc}(k)}||$ and $||\mathbf{Q}^{\mathtt{ref}(k)}||$) [2]. In this sense, the parameter $\mathcal{E}_s$ appears as a measure of the relative errors induced when approximating the vectors of displacements $\mathbf{q}^{(k)}$ and forces $\mathbf{F}^{(k)}$ by means of a reduced wave basis (cf. Eqs. (17) and (18)) [3]. As a result, reducing $\mathcal{E}_s$ is the key idea behind the wave mode selection strategy.

3.3.3. Features of the error bound $\mathcal{E}_s$

Considering Eq. (62), the WFE reduced formulation involves two kinds of errors for expressing the vectors of displacements and forces. The first one is linked to $(\epsilon_1^{\mathbf{E}} + \epsilon_2^{\mathbf{E}})$ and $(\epsilon_1^{\mathbf{E}^\star} + \epsilon_2^{\mathbf{E}^\star})$, say for approximating the vectors $\mathbf{E}_s$ and $\mathbf{E}_s^\star$

---

[2] A justification of this statement follows from the discussions in Section 3.3.1.

[3] It is worth emphasizing that the computation of the vectors of wave amplitudes follows from the matrix formulation (15), considering a reduced wave basis $\{\widetilde{\mathbf{\Phi}}_j\}_j$ instead of the full wave basis $\{\mathbf{\Phi}_j\}_j$.

by means of the reduced vectors $\widetilde{\mathbf{E}}_s$ and $\widetilde{\mathbf{E}}_s^\star$; the second one is linked to $(\epsilon_1^{\mathbf{A}} + \epsilon_2^{\mathbf{A}})$ and $(\epsilon_1^{\mathbf{A}^\star} + \epsilon_2^{\mathbf{A}^\star})$, say for approximating the matrices $\mathbf{A}^s$ and $\mathbf{A}^{\star s}$ by means of the reduced matrices $\widetilde{\mathbf{A}}^s$ and $\widetilde{\mathbf{A}}^{\star s}$.

When $s \to \infty$, since $\rho(\mathbf{A}) < 1$ and $\rho(\mathbf{A}^\star) < 1$ (Assumption 1) and thus $\lim_{s\to\infty} ||\mathbf{A}^s|| = \lim_{s\to\infty} ||\mathbf{A}^{\star s}|| = 0$, it appears that $\mathcal{E}_s \to \mathcal{E}_\infty = \max\{(\epsilon_1^{\mathbf{E}} + \epsilon_2^{\mathbf{E}}), (\epsilon_1^{\mathbf{E}^\star} + \epsilon_2^{\mathbf{E}^\star})\}$. In this case, $\mathbf{E}_s$ and $\mathbf{E}_s^\star$ converge to the vectors of wave amplitudes $\mathbf{Q}^{\mathtt{ref}\star}$ and $\mathbf{Q}^{\mathtt{ref}}$ (a proof of this statement readily follows from Eq. (38), considering that $\mathbf{E}_s = \mathbf{E}_s^{(1)}$ and $\mathbf{Q}^{\mathtt{ref}\star} = \mathbf{Q}^{\mathtt{inc}(1)}$). Then the minimization problem is to approximate the vectors $\mathbf{Q}^{\mathtt{ref}\star}$ and $\mathbf{Q}^{\mathtt{ref}}$ explicitly by means of the reduced vectors $\widetilde{\mathbf{Q}}^{\mathtt{ref}\star}$ and $\widetilde{\mathbf{Q}}^{\mathtt{ref}}$. In particular, the problem is to reduce the contribution of the residual wave modes, i.e. $||\mathcal{L}_{\mathtt{r}}\mathbf{Q}^{\mathtt{ref}\star}||$ and $||\mathcal{L}_{\mathtt{r}}\mathbf{Q}^{\mathtt{ref}}||$, for reducing the relative errors $\epsilon_2^{\mathbf{E}}$ and $\epsilon_2^{\mathbf{E}^\star}$ (cf. Eq. (51)). The solution consists in increasing the number m of retained wave modes so as to reduce the norms $||\mathcal{L}_{\mathtt{r}}\mathbf{Q}^{\mathtt{ref}\star}||$ and $||\mathcal{L}_{\mathtt{r}}\mathbf{Q}^{\mathtt{ref}}||$ until they reach an arbitrary small threshold (this is understood since these norms are decreasing functions of m) [4]. The drawback of this procedure is that no rigorous criterion exists to define this threshold exactly, which makes the strategy inefficient for selecting precisely which wave modes are to be retained.

On the other hand, Eq. (62) states that $(\epsilon_1^{\mathbf{A}} + \epsilon_2^{\mathbf{A}})$ and $(\epsilon_1^{\mathbf{A}^\star} + \epsilon_2^{\mathbf{A}^\star})$ have to be considered as additional sources of errors when s is not too large. Unlike the case when $s \to \infty$, the minimization of $\mathcal{E}_s$ appears not necessarily linked to an increase of the number m of retained modes. For instance, the term $||\widetilde{\mathbf{A}}^s\widetilde{\mathcal{L}} - \widetilde{\mathcal{L}}\mathbf{A}^s||$ used for expressing $\epsilon_1^{\mathbf{A}}$ does not appear necessarily as a decreasing function of m. On the contrary, once the components of the matrix $\widetilde{\mathbf{A}}^s\widetilde{\mathcal{L}}$ appear close to those of the matrix $\widetilde{\mathcal{L}}\mathbf{A}^s$ – that is to say, when an optimal reduced wave basis has been found –, every additional increase of the size of these matrices will induce an increase

---

[4]Indeed, the size of $\mathcal{L}_{\mathtt{r}}$ is linked to $n - m$ while the vectors $\mathbf{Q}^{\mathtt{ref}\star}$ and $\mathbf{Q}^{\mathtt{ref}}$ do not depend on m.

of the error bound $\mathcal{E}_s$. From this point of view, $\mathcal{E}_s$ appears sensitive when the size of the wave basis is overestimated. This is the important feature of the proposed MOR strategy. As a result, the issue is to manage a global minimization problem among $(\epsilon_1^{\mathbf{E}} + \epsilon_2^{\mathbf{E}})$ (resp. $(\epsilon_1^{\mathbf{E}^\star} + \epsilon_2^{\mathbf{E}^\star})$) and $(\epsilon_1^{\mathbf{A}} + \epsilon_2^{\mathbf{A}})$ (resp. $(\epsilon_1^{\mathbf{A}^\star} + \epsilon_2^{\mathbf{A}^\star})$), for a given integer s. The error bound $\mathcal{E}_s$ is much more restrictive than $\mathcal{E}_\infty$ in the sense that it provides a clear answer for the number of wave modes that have to be retained. This enables the selection of wave modes to be carried out in a quite qualitative way, the required number of wave modes being exactly determined by seeking a minimum value of $\mathcal{E}_s$, i.e. for a particular reduced wave basis whose size is not necessarily equal to the size of the full wave basis.

3.4. Selection of the wave modes

3.4.1. Introduction

The strategy for selecting the contributing wave modes is detailed as follows. The key idea is to rank the wave modes in a preliminary step (see Section 3.4.3), and then to plot the error bound $\mathcal{E}_s$ as a function of the number m of retained wave modes (i.e. the first m wave modes as ranked in this preliminary step). As a result, the strategy aims at identifying this number of retained wave modes which corresponds to a minimum value of this function $m \mapsto \mathcal{E}_s$ (the existence of such a minimum follows from the comments in Section 3.3.3). For this task, the assumptions $||\widetilde{\mathbf{A}}^s|| \leq ||\mathbf{A}^s||$ as well as $||\widetilde{\mathbf{A}}^{\star s}|| \leq ||\mathbf{A}^{\star s}||$ need to be satisfied (Assumption 2), while it is assumed that $\rho(\mathbf{A}) < 1$ as well as $\rho(\mathbf{A}^\star) < 1$ (Assumption 1). These assumptions enable the error norms $||\widetilde{\mathbf{q}}^{(k)} - \mathbf{q}^{(k)}||$ and $||\widetilde{\mathbf{F}}^{(k)} - \mathbf{F}^{(k)}||$ to be bounded as in Eqs. (64) and (65). It is worth recalling that Assumption 1 is satisfied provided that the number of substructures, or the waveguide damping, is high enough (cf. comments below Assumption 1); also, Assumption 2 appears to be satisfied

when $\mathcal{E}_s$ is small enough (cf. comments below Assumption 2).

It is worth emphasizing that $\mathcal{E}_s$ depends on the integer s (i.e. the number of forward and backward passings of waves along the waveguide), while it is frequency dependent. Choosing an appropriate integer s and an appropriate frequency for expressing $\mathcal{E}_s$ as a function of the number m of retained wave modes only, appears as a crucial task to undertake the minimization problem with less effort (e.g. regardless of the discrete frequencies considered within the studied frequency band). Such an issue is addressed hereafter.

3.4.2. Expression of the error bound $\mathcal{E}_s$

Choice of the integer s

The magnitude of the error bound $\mathcal{E}_s$ is linked to $(\epsilon_1^{\mathbf{E}} + \epsilon_2^{\mathbf{E}})$ and $(\epsilon_1^{\mathbf{A}} + \epsilon_2^{\mathbf{A}})$, as well as $(\epsilon_1^{\mathbf{E}^\star} + \epsilon_2^{\mathbf{E}^\star})$ and $(\epsilon_1^{\mathbf{A}^\star} + \epsilon_2^{\mathbf{A}^\star})$ (cf. Eq. (62)). Additionally, it depends on the magnitudes of $||\mathbf{A}^s||/(1 - ||\mathbf{A}^s||)$ and $(1 + ||\mathbf{A}^s||)/(1 - ||\mathbf{A}^s||)$, as well as the magnitudes of $(||\mathbf{A}^{\star s}||)/(1 - ||\mathbf{A}^{\star s}||)$ and $(1 + ||\mathbf{A}^{\star s}||)/(1 - ||\mathbf{A}^{\star s}||)$. Choosing an integer s high enough so that these magnitudes are small enough is a crucial task for computing small values of $\mathcal{E}_s$ (i.e. if one aims at stating that the reduced model is accurate for predicting the dynamic behavior of the waveguide). However, s has to be small enough if one requires $(\epsilon_1^{\mathbf{A}} + \epsilon_2^{\mathbf{A}})$ and $(\epsilon_1^{\mathbf{A}^\star} + \epsilon_2^{\mathbf{A}^\star})$ to impact significantly the magnitude of $\mathcal{E}_s$ (see discussions in Section 3.3.3). As a rule of thumb, it is proposed to choose s such that $||\mathbf{A}^s|| \approx 0.1$ and $||\mathbf{A}^{\star s}|| \approx 0.1$. The motivation behind this choice is that $(1 + ||\mathbf{A}^s||)/(1 - ||\mathbf{A}^s||)$ and $(1 + ||\mathbf{A}^{\star s}||)/(1 - ||\mathbf{A}^{\star s}||)$ are enabled to be close to one, i.e. without overestimating $\mathcal{E}_s$. As a result, it is proposed to seek the integer s as

$$s = \max \left\{ u \geq \max\{s_0, s_0^\star\} : ||\mathbf{A}^u|| \geq 0.1 \ , \ ||\mathbf{A}^{\star u}|| \geq 0.1 \right\}. \tag{66}$$

Choice of the frequency

The error bound $\mathcal{E}_s$ (cf. Eq. (62)) is to be expressed at several discrete frequencies, i.e. over the frequency band where the forced response is to be computed. To address this issue, it is proposed to consider the highest frequency only, where $\mathcal{E}_s$ is likely to reach its maximum value. This is explained since a maximum number of wave modes are expected to contribute to the forced response, which means that vectors $\mathbb{F}$, $\mathbb{F}^\star$ and matrices $\mathbb{C}$, $\mathbb{C}^\star$ (cf. Eq. (12)) are expected to have a maximum number of non-zero components (in other words, error norms for these vectors and matrices are expected to be large); the same conclusion holds for the vectors $\mathbf{E}_s$, $\mathbf{E}_s^\star$ and the matrices $\mathbf{A}^s$, $\mathbf{A}^{\star s}$, since they are expressed by means of $\mathbb{F}$, $\mathbb{F}^\star$, $\mathbb{C}$ and $\mathbb{C}^\star$ (see Section 3.3.1). This means that the relative errors $\epsilon_1^{\mathbf{E}}$, $\epsilon_2^{\mathbf{E}}$, $\epsilon_1^{\mathbf{A}}$ and $\epsilon_2^{\mathbf{A}}$, as well as $\epsilon_1^{\mathbf{E}^\star}$, $\epsilon_2^{\mathbf{E}^\star}$, $\epsilon_1^{\mathbf{A}^\star}$ and $\epsilon_2^{\mathbf{A}^\star}$, are expected to be maximum.

To summarize, it is proposed to assess the error norms $||\widetilde{\mathbf{q}}^{(k)} - \mathbf{q}^{(k)}||$ and $||\widetilde{\mathbf{F}}^{(k)} - \mathbf{F}^{(k)}||$ (see Eqs. (64) and (65)), at any discrete frequency considered within the studied frequency band, by means of the bound $\mathcal{E}_s$ formulated at the maximum discrete frequency (considered within that frequency band) only.

3.4.3. Minimization of the error bound $\mathcal{E}_s$

As mentioned in Section 3.4.1, the key idea behind the minimization procedure of the error bound $\mathcal{E}_s$ is to rank the wave modes in a preliminary step. This procedure enables $\mathcal{E}_s$ to be considered as a function of the single variable m (i.e. the first m wave modes as ranked in this preliminary step) for $1 \leq m \leq n$, where n is the total number of incident / reflected wave modes contained in the full wave

basis. This procedure yields the minimization of $\mathcal{E}_s$ to be an easy task – indeed, this requires us to plot the function $m \mapsto \mathcal{E}_s$ and to identify its minimum value – which is weakly expensive from the computational point of view [5]. The fact that such a minimum value is likely to occur follows from the comments in Section 3.3.3.

Ranking the wave modes (as previously explained) efficiently appears as a key issue to accelerate the convergence of the WFE reduced model when the number m of retained wave modes increases. In other words, the objective behind the ranking procedure is to find a minimum value of $\mathcal{E}_s$ which corresponds to a small value of m, say a reduced basis of small size. This task requires us to provide a rough estimate on how the wave modes are expected to contribute to the forced response. A relevant solution is to rank the wave modes with respect to the magnitudes of the components of the vectors $\mathbf{E}_s$ and $\mathbf{E}_s^\star$ – denoted as $\{\mathbf{E}_{sj}\}_j$ and $\{\mathbf{E}_{sj}^\star\}_j$, respectively – as this yields the relative errors $\epsilon_2^{\mathbf{E}}$ and $\epsilon_2^{\mathbf{E}^\star}$ to be strongly decreasing functions of m (a justification of this statement follows from the discussions in Section 3.3.3).

Then the strategy for selecting the wave modes can be stated as follows:

1. Check that $\rho(\mathbf{A}) < 1$ and $\rho(\mathbf{A}^\star) < 1$ (Assumption 1); if not, try to increase the number of substructures or the waveguide damping;

2. Choose the integer s according to Eq. (66);

3. Rank the wave modes with respect to the magnitudes of the components $\{\mathbf{E}_{sj}\}_j \cup \{\mathbf{E}_{sj}^\star\}_j$;

4. Compute the error bound $\mathcal{E}_s$ by means of Eq. (62) at the highest frequency considered within the studied frequency band, as a function of m (i.e. the first m wave modes as ranked in step 3);

---

[5]In fact, the procedure requires us to compute $\mathcal{E}_s$ n times only (i.e. for $1 \leq m \leq n$), i.e. to compute $\mathcal{E}_s$ one single time for a given m without scanning all the possible families of m wave modes for expressing $\mathcal{E}_s$.

5. Define the domain of validity of $\mathcal{E}_s$, i.e. when $||\widetilde{\mathbf{A}}^s|| \leq ||\mathbf{A}^s||$ and $||\widetilde{\mathbf{A}}^{\star s}|| \leq ||\mathbf{A}^{\star s}||$ (Assumption 2);

6. Identify the minimum value of $\mathcal{E}_s$.

4. Application to coupled waveguides

4.1. Preliminary comments

The case of two waveguides 1 and 2 connected to an elastic junction, free from excitation sources, is investigated (see Figure 1(d)). Following the WFE framework (see Section 2.1), it is proposed to assess the behavior of each waveguide i ($i = 1, 2$) by means of wave modes $\{(\mu_j)_i, (\boldsymbol{\Phi}_j)_i\}_{j=1,\ldots,2n_i}$. Also, it is proposed to model the coupling junction by means of the matrix $\mathbb{C}$ described in Eq. (13). In this sense, the relationships between the vectors of reflected and incident wave amplitudes, at coupling interfaces, can be expressed as

$$\mathbf{Q}_i^{\texttt{ref}} = \sum_{r=1}^{2} \mathbb{C}_{ir} \mathbf{Q}_r^{\texttt{inc}} \qquad i = 1, 2. \tag{67}$$

Here, the reflected wave modes (denoted by means of the superscript $\texttt{ref}$) are to be understood as the waves traveling outward from the junction, i.e. which are induced by the incident wave modes for both waveguides i and r.

Apart from the coupling conditions, considering the other boundaries of waveguides 1 and 2 e.g. where forces or displacements can be applied, the relationships between the vectors of reflected and incident wave amplitudes are quite similar to Eq. (12), i.e.

$$\mathbf{Q}_i^{\texttt{ref}\star} = \mathbb{C}_i^{\star} \mathbf{Q}_i^{\texttt{inc}\star} + \mathbb{F}_i^{\star} \qquad i = 1, 2. \tag{68}$$

34

4.2. Error norms

The idea behind the MOR strategy is to approximate the vectors of displacements $\mathbf{q}_i^{(k_i)}$ and internal forces $\mathbf{F}_i^{(k_i)}$ of each waveguide i ($i = 1, 2$), over any substructure boundary k_i ($k_i = 1, \ldots, N_i + 1$, N_i being the number of substructures used for describing the waveguide i) by means of a reduced wave basis $\{(\widetilde{\boldsymbol{\Phi}}_j)_i\}_{j=1,\ldots,2m_i}$ (with a same number $m_i \leq n_i$ of incident and reflected modes). In this framework, the aim is to compute the forced response of the coupled structure using a reduced matrix formulation of small size $2(m_1 + m_2)$ compared to the conventional matrix formulation (whose size is $2(n_1 + n_2)$) obtained when the full wave bases are considered (cf Eq. (16)). The related errors can be readily derived on a same scheme as for Eqs. (26) and (27), i.e.

$$\left\| \begin{bmatrix} \widetilde{\mathbf{q}}_1^{(k_1)} - \mathbf{q}_1^{(k_1)} \\ \widetilde{\mathbf{q}}_2^{(k_2)} - \mathbf{q}_2^{(k_2)} \end{bmatrix} \right\| \leq \|\boldsymbol{\Phi}_{\mathtt{q}}^{\mathtt{inc}}\| \left(\left\| \begin{bmatrix} \Delta\mathbf{Q}_1^{\mathtt{inc}(k_1)} \\ \Delta\mathbf{Q}_2^{\mathtt{inc}(k_2)} \end{bmatrix} \right\| + \left\| \begin{bmatrix} \Delta\mathbf{Q}_1^{\mathtt{ref}(k_1)} \\ \Delta\mathbf{Q}_2^{\mathtt{ref}(k_2)} \end{bmatrix} \right\| \right)$$
$$k_1 = 1, \ldots, N_1 + 1 \qquad k_2 = 1, \ldots, N_2 + 1, \quad (69)$$

and

$$\left\| \begin{bmatrix} \widetilde{\mathbf{F}}_1^{(k_1)} - \mathbf{F}_1^{(k_1)} \\ \widetilde{\mathbf{F}}_2^{(k_2)} - \mathbf{F}_2^{(k_2)} \end{bmatrix} \right\| \leq \|\boldsymbol{\Phi}_{\mathtt{F}}^{\mathtt{inc}}\| \left(\left\| \begin{bmatrix} \Delta\mathbf{Q}_1^{\mathtt{inc}(k_1)} \\ \Delta\mathbf{Q}_2^{\mathtt{inc}(k_2)} \end{bmatrix} \right\| + \left\| \begin{bmatrix} \Delta\mathbf{Q}_1^{\mathtt{ref}(k_1)} \\ \Delta\mathbf{Q}_2^{\mathtt{ref}(k_2)} \end{bmatrix} \right\| \right)$$
$$k_1 = 1, \ldots, N_1 + 1 \qquad k_2 = 1, \ldots, N_2 + 1, \quad (70)$$

where $\boldsymbol{\Phi}_{\mathtt{q}}^{\mathtt{inc}}$ and $\boldsymbol{\Phi}_{\mathtt{F}}^{\mathtt{inc}}$ are square $(n_1 + n_2) \times (n_1 + n_2)$ matrices defined as

$$\boldsymbol{\Phi}_{\mathtt{q}}^{\mathtt{inc}} = \begin{bmatrix} (\boldsymbol{\Phi}_{\mathtt{q}}^{\mathtt{inc}})_1 & \mathbf{0} \\ \mathbf{0} & (\boldsymbol{\Phi}_{\mathtt{q}}^{\mathtt{inc}})_2 \end{bmatrix} \quad , \quad \boldsymbol{\Phi}_{\mathtt{F}}^{\mathtt{inc}} = \begin{bmatrix} (\boldsymbol{\Phi}_{\mathtt{F}}^{\mathtt{inc}})_1 & \mathbf{0} \\ \mathbf{0} & (\boldsymbol{\Phi}_{\mathtt{F}}^{\mathtt{inc}})_2 \end{bmatrix}. \quad (71)$$

In Eqs. (69) and (70), $\Delta\mathbf{Q}_i^{\mathtt{inc}(k_i)}$ and $\Delta\mathbf{Q}_i^{\mathtt{ref}(k_i)}$ ($i = 1, 2$) are expressed as $\Delta\mathbf{Q}_i = \widetilde{\mathcal{L}}_i^T \widetilde{\mathbf{Q}}_i - \mathbf{Q}_i$, where $\widetilde{\mathcal{L}}_i$ is an $m_i \times n_i$ incidence matrix such that $\widetilde{\mathcal{L}}_i^T$ is unitary (cf.

Section 2.4.2). Considering as in Section 2.4.2 a $(n_i - m_i) \times n_i$ incidence matrix $\mathcal{L}_{\mathbf{r}i}$ – such that $\mathcal{L}_{\mathbf{r}i}^T$ is unitary and $\mathcal{L}_{\mathbf{r}i}^T \mathcal{L}_{\mathbf{r}i} + \widetilde{\mathcal{L}}_i^T \widetilde{\mathcal{L}}_i = \mathbf{I}_{n_i} \ \forall i$ (cf. above Proposition 1) – yields the error norms on the right hand sides of Eqs. (69) and (70) to be bounded as (cf. Eq. (28))

$$\left\| \begin{bmatrix} \Delta \mathbf{Q}_1 \\ \Delta \mathbf{Q}_2 \end{bmatrix} \right\| \leq \left\| \begin{bmatrix} \widetilde{\mathbf{Q}}_1 \\ \widetilde{\mathbf{Q}}_2 \end{bmatrix} - \widetilde{\mathcal{L}} \begin{bmatrix} \mathbf{Q}_1 \\ \mathbf{Q}_2 \end{bmatrix} \right\| + \left\| \mathcal{L}_{\mathbf{r}} \begin{bmatrix} \mathbf{Q}_1 \\ \mathbf{Q}_2 \end{bmatrix} \right\|, \tag{72}$$

where $\widetilde{\mathcal{L}}$ and $\mathcal{L}_{\mathbf{r}}$ are $(m_1 + m_2) \times (n_1 + n_2)$ and $(n_1 - m_1 + n_2 - m_2) \times (n_1 + n_2)$ matrices, respectively, defined as

$$\widetilde{\mathcal{L}} = \begin{bmatrix} \widetilde{\mathcal{L}}_1 & \mathbf{0} \\ \mathbf{0} & \widetilde{\mathcal{L}}_2 \end{bmatrix} \quad , \quad \mathcal{L}_{\mathbf{r}} = \begin{bmatrix} \mathcal{L}_{\mathbf{r}1} & \mathbf{0} \\ \mathbf{0} & \mathcal{L}_{\mathbf{r}2} \end{bmatrix}. \tag{73}$$

The derivation of Eq. (72) is based on the fact that both $\widetilde{\mathcal{L}}^T$ and $\mathcal{L}_{\mathbf{r}}^T$ are unitary matrices [6]. As suggested in Section 3.2, further derivation of the bound proposed by Eq. (72) is achieved by expressing the vectors of wave amplitudes $\mathbf{Q}_i^{\texttt{inc}(k_i)}$ and $\mathbf{Q}_i^{\texttt{ref}(k_i)}$ $(i = 1, 2)$ in a suitable way. Using the methodology depicted in Section 3.2 while considering Eqs. (67) and (68) leads to

$$\mathbf{Q}_i^{\texttt{inc}(k_i)} = \boldsymbol{\mu}_i^{k_i-1} \left[\mathbb{C}_i^\star \boldsymbol{\mu}_i^{N_i} \sum_{r=1}^{2} \left(\mathbb{C}_{ir} \boldsymbol{\mu}_r^{N_r-(k_r-1)} \mathbf{Q}_r^{\texttt{inc}(k_r)} \right) + \mathbb{F}_i^\star \right]$$
$$k_i = 1, \ldots, N_i + 1 \qquad i = 1, 2, \tag{74}$$

and

$$\mathbf{Q}_i^{\texttt{ref}(k_i)} = \boldsymbol{\mu}_i^{N_i-(k_i-1)} \sum_{r=1}^{2} \left(\mathbb{C}_{ir} \boldsymbol{\mu}_r^{N_r} \left[\mathbb{C}_r^\star \boldsymbol{\mu}_r^{k_r-1} \mathbf{Q}_r^{\texttt{ref}(k_r)} + \mathbb{F}_r^\star \right] \right)$$
$$k_i = 1, \ldots, N_i + 1 \qquad i = 1, 2, \tag{75}$$

where $\boldsymbol{\mu}_i$ is the diagonal matrix of the wave mode parameters $\{(\mu_j^{\texttt{inc}})_i\}_j$, defined such that $\|\boldsymbol{\mu}_i\| < 1$. Following the discussion in Section 3.3.1 while considering

---

[6]This statement is readily proved since the matrices $\widetilde{\mathcal{L}}_i^T$ and $\mathcal{L}_{\mathbf{r}i}^T$ are unitary $\forall i$.

Eqs. (74) and (75), it is proposed to assess the errors $\Delta \mathbf{Q}_i^{\mathtt{inc}(k_i)}$ and $\Delta \mathbf{Q}_i^{\mathtt{ref}(k_i)}$ $(i = 1, 2)$ as

$$\left\| \begin{bmatrix} \Delta \mathbf{Q}_1^{\mathtt{inc}(k_1)} \\ \Delta \mathbf{Q}_2^{\mathtt{inc}(k_2)} \end{bmatrix} \right\| \leq \|\Delta \mathbf{Q}^{\mathtt{ref}\star}\| \quad , \quad \left\| \begin{bmatrix} \Delta \mathbf{Q}_1^{\mathtt{ref}(k_1)} \\ \Delta \mathbf{Q}_2^{\mathtt{ref}(k_2)} \end{bmatrix} \right\| \leq \|\Delta \mathbf{Q}^{\mathtt{ref}}\| \qquad \forall (k_1, k_2), \tag{76}$$

where

$$\Delta \mathbf{Q}^{\mathtt{ref}\star} = \begin{bmatrix} \Delta \mathbf{Q}_1^{\mathtt{inc}(1)} \\ \Delta \mathbf{Q}_2^{\mathtt{inc}(1)} \end{bmatrix} \quad , \quad \Delta \mathbf{Q}^{\mathtt{ref}} = \begin{bmatrix} \Delta \mathbf{Q}_1^{\mathtt{ref}(N_1+1)} \\ \Delta \mathbf{Q}_2^{\mathtt{ref}(N_2+1)} \end{bmatrix}. \tag{77}$$

Here, $\Delta \mathbf{Q}^{\mathtt{ref}\star}$ refers to the error for the vectors of reflected wave amplitudes at the left boundaries of the waveguides – i.e. when $k_1 = 1$ and $k_2 = 1$ – where forces and displacements are prescribed; also, $\Delta \mathbf{Q}^{\mathtt{ref}}$ refers to the error for the vectors of reflected wave amplitudes at the right boundaries of the waveguides – i.e. when $k_1 = N_1 + 1$ and $k_2 = N_2 + 1$ – where coupling conditions are considered. According to Section 3.2, bounds of $\|\Delta \mathbf{Q}^{\mathtt{ref}\star}\|$ and $\|\Delta \mathbf{Q}^{\mathtt{ref}}\|$ are derived from the consideration of the following vectors of wave amplitudes $\mathbf{Q}^{\mathtt{ref}\star}$ and $\mathbf{Q}^{\mathtt{ref}}$:

$$\mathbf{Q}^{\mathtt{ref}\star} = \begin{bmatrix} \mathbf{Q}_1^{\mathtt{inc}(1)} \\ \mathbf{Q}_2^{\mathtt{inc}(1)} \end{bmatrix} \quad , \quad \mathbf{Q}^{\mathtt{ref}} = \begin{bmatrix} \mathbf{Q}_1^{\mathtt{ref}(N_1+1)} \\ \mathbf{Q}_2^{\mathtt{ref}(N_2+1)} \end{bmatrix}. \tag{78}$$

These vectors are readily expressed from Eqs. (74) and (75) as

$$\mathbf{Q}^{\mathtt{ref}\star} = \mathbf{A}\mathbf{Q}^{\mathtt{ref}\star} + \mathbf{B} \quad , \quad \mathbf{Q}^{\mathtt{ref}} = \mathbf{A}^\star \mathbf{Q}^{\mathtt{ref}} + \mathbf{B}^\star, \tag{79}$$

where

$$\mathbf{A} = \begin{bmatrix} \mathbb{C}_1^\star \boldsymbol{\mu}_1^{N_1} \mathbb{C}_{11} \boldsymbol{\mu}_1^{N_1} & \mathbb{C}_1^\star \boldsymbol{\mu}_1^{N_1} \mathbb{C}_{12} \boldsymbol{\mu}_2^{N_2} \\ \mathbb{C}_2^\star \boldsymbol{\mu}_2^{N_2} \mathbb{C}_{21} \boldsymbol{\mu}_1^{N_1} & \mathbb{C}_2^\star \boldsymbol{\mu}_2^{N_2} \mathbb{C}_{22} \boldsymbol{\mu}_2^{N_2} \end{bmatrix} \quad , \quad \mathbf{B} = \begin{bmatrix} \mathbb{F}_1^\star \\ \mathbb{F}_2^\star \end{bmatrix}, \tag{80}$$

and

$$\mathbf{A}^\star = \begin{bmatrix} \mathbb{C}_{11} \boldsymbol{\mu}_1^{N_1} \mathbb{C}_1^\star \boldsymbol{\mu}_1^{N_1} & \mathbb{C}_{12} \boldsymbol{\mu}_2^{N_2} \mathbb{C}_2^\star \boldsymbol{\mu}_2^{N_2} \\ \mathbb{C}_{21} \boldsymbol{\mu}_1^{N_1} \mathbb{C}_1^\star \boldsymbol{\mu}_1^{N_1} & \mathbb{C}_{22} \boldsymbol{\mu}_2^{N_2} \mathbb{C}_2^\star \boldsymbol{\mu}_2^{N_2} \end{bmatrix} \quad , \quad \mathbf{B}^\star = \begin{bmatrix} \mathbb{C}_{11} \boldsymbol{\mu}_1^{N_1} \mathbb{F}_1^\star + \mathbb{C}_{12} \boldsymbol{\mu}_2^{N_2} \mathbb{F}_2^\star \\ \mathbb{C}_{21} \boldsymbol{\mu}_1^{N_1} \mathbb{F}_1^\star + \mathbb{C}_{22} \boldsymbol{\mu}_2^{N_2} \mathbb{F}_2^\star \end{bmatrix}.$$

Bounds of the error norms $||\Delta\mathbf{Q}^{\mathtt{ref}\star}||$ and $||\Delta\mathbf{Q}^{\mathtt{ref}}||$ result directly from Eqs. (47) and (49), $\mathbf{E}_s$ and $\mathbf{E}_s^\star$ being expressed as in Eqs. (45) and (50). It is worth recalling that these bounds remain valid provided that $\rho(\mathbf{A}) < 1$ and $\rho(\mathbf{A}^\star) < 1$ (Assumption 1), while integers s_0 and $s_0^\star$ (cf. Eqs. (47) and (49)) are to be considered such that $||\mathbf{A}^s|| < 1$ for $s \geq s_0$ and $||\mathbf{A}^{\star s}|| < 1$ for $s \geq s_0^\star$.

As a result, a bound of $||\Delta\mathbf{Q}^{\mathtt{ref}\star}|| + ||\Delta\mathbf{Q}^{\mathtt{ref}}||$ follows directly from Eq. (63). It appears to be linked to the error bound $\mathcal{E}_s$ previously defined in Eq. (62), provided that $||\widetilde{\mathbf{A}}^s|| \leq ||\mathbf{A}^s||$ and $||\widetilde{\mathbf{A}}^{\star s}|| \leq ||\mathbf{A}^{\star s}||$ (Assumption 2). Also, the bounds of $||\widetilde{\mathbf{q}}^{(k)} - \mathbf{q}^{(k)}||$ and $||\widetilde{\mathbf{F}}^{(k)} - \mathbf{F}^{(k)}||$ result from Eqs. (64) and (65).

4.3. Selection of the wave modes

The selection of the wave modes for both waveguides 1 and 2 can be achieved by considering the procedure depicted in Section 3.4. To address this task, it is proposed to express the error bound $\mathcal{E}_s$ as a function of a single variable m, i.e. the number of incident / reflected wave modes retained for both waveguides 1 and 2. In other words, it is proposed to assess the behavior of the waveguides using two reduced wave bases $\{(\widetilde{\boldsymbol{\Phi}}_j)_1\}_j$ and $\{(\widetilde{\boldsymbol{\Phi}}_j)_2\}_j$ of same size $2m$, where $m = m_1 = m_2$.

As suggested in Section 3.4, the wave modes are to be ranked before undertaking the minimization of $\mathcal{E}_s$. This procedure enables the error bound $\mathcal{E}_s$ to be considered as a function of the single variable m (i.e. the first m wave modes for both waveguides 1 and 2, as ranked by the proposed procedure) whose minimum value yields the number of wave modes to be retained. This ranking procedure can be done independently for each waveguide, considering the components of the

vectors $\mathbf{E}_s$ and $\mathbf{E}_s^\star$ that exhibit the largest magnitudes. In the present framework, these vectors are expressed as

$$\mathbf{E}_s = \left[\begin{array}{c} \mathbf{E}_{s1} \\ \mathbf{E}_{s2} \end{array} \right] \quad , \quad \mathbf{E}_s^\star = \left[\begin{array}{c} \mathbf{E}_{s1}^\star \\ \mathbf{E}_{s2}^\star \end{array} \right], \tag{82}$$

where $\mathbf{E}_{si}$ and $\mathbf{E}_{si}^\star$ are $n_i \times 1$ vectors associated to waveguide i ($i = 1, 2$). Thus, the issue is to rank the wave modes of each waveguide i with respect to the magnitudes of the components of $\mathbf{E}_{si}$ and $\mathbf{E}_{si}^\star$ – denoted as $\{(\mathbf{E}_{sj})_i\}_j$ and $\{(\mathbf{E}_{sj}^\star)_i\}_j$, respectively. As discussed in Section 3.4, this procedure enables the relative errors $\epsilon_2^{\mathbf{E}}$ and $\epsilon_2^{\mathbf{E}^\star}$ to be considered as strongly decreasing functions of m. This yields the convergence of the WFE formulation to be improved by considering reduced wave bases of small size, constituted from the wave modes that efficiently contribute to the dynamic behavior of the structure.

To summarize, the strategy for selecting the wave modes can be stated as follows:

1. Check that $\rho(\mathbf{A}) < 1$ and $\rho(\mathbf{A}^\star) < 1$ (Assumption 1); if not, try to increase the number of substructures (for each waveguide) or the waveguide damping;

2. Choose integer s according to Eq. (66);

3. Rank the wave modes of each waveguide i ($i = 1, 2$) with respect to the magnitudes of the components $\{(\mathbf{E}_{sj})_i\}_j \cup \{(\mathbf{E}_{sj}^\star)_i\}_j$;

4. Compute the error bound $\mathcal{E}_s$ by means of Eq. (62) at the highest frequency considered within the studied frequency band, as a function of m (i.e. the first m wave modes for both waveguides 1 and 2, as ranked in step 3);

5. Define the domain of validity of $\mathcal{E}_s$, i.e. when $||\widetilde{\mathbf{A}}^s|| \leq ||\mathbf{A}^s||$ and $||\widetilde{\mathbf{A}}^{\star s}|| \leq ||\mathbf{A}^{\star s}||$ (Assumption 2);

6. Identify the minimum value of $\mathcal{E}_s$.

39

5. Numerical experiments

5.1. Validation of the MOR strategy

Let us consider the waveguides depicted in Figure 1, i.e.

- a clamped beam-like structure with thick cross-section whose left end is subjected to a uniform transverse force field (Figure 1(a));

- a Reissner-Mindlin plate with one edge subjected to a prescribed transverse displacement (Figure 1(b));

- a clamped sandwich beam with soft core and stiff skins whose left end (bottom skin only) is subjected to a uniform transverse force field (Figure 1(c));

- two beam-like structures coupled with an elastic junction over one of their boundaries, the other boundaries being respectively clamped and subjected to a uniform transverse force field (Figure 1(d)).

The WFE matrix formulations for computing the forced response of such waveguides are expressed by Eqs. (15) and (16) (see also ref. [1]). The relevance of these formulations has been proved provided a sufficient number of wave modes has been considered [1]. The classic model reduction strategy consists in retaining the wave modes whose wavenumbers – computed at the smallest frequency considered within the involved frequency band – exhibit the smallest imaginary parts. This turns out to be similar to retaining the wave modes for which the wave parameters $\{\widetilde{\mu}_j\}_j$ (see Section 2) have the magnitudes that are closest to one. Following this procedure, the frequency response functions of waveguides can be drawn as shown in Figure 3(a-d), considering as number of incident / reflected wave modes e.g. $m = 30$ for the beam, $m = 60$ for the plate, $m = 80$ for the sandwich structure and $m = 30$ for the coupled system (say for each of the connected waveguides).

40

The WFE solutions are compared to conventional FE solutions involving the full discretized models of the waveguides (cf. Figure 3). For this task, the quadratic velocity of each waveguide [7] at one measurement point (located in the excitation area for the beam-like and sandwich structures; located in the middle of the free left boundary for the plate) has been considered. Clearly, it is shown that the WFE formulation suffers from a lack of convergence at high frequencies for predicting the structure resonances and anti-resonances. To solve this issue, the sizes of the wave bases need to be enlarged. The drawback of this approach is that a large number of wave modes can be taken into account, even if part of these modes weakly contribute for expressing the forced responses. This is explained since the selection of the wave mode is carried out in accordance to the magnitudes of the wave parameters $\{\widetilde{\mu}_j\}_j$ (see above), i.e. considering only the way the wave modes are propagating at a certain frequency (regardless of their contribution for describing the boundary conditions of the waveguides).

Figure 3

In contrast, the MOR strategy based on the minimization of the error bound $\mathcal{E}_s$ (Eq. (62)) yields an efficient means for selecting the wave modes that effectively contribute to the forced response, irrespective of the magnitudes of the wave parameters $\{\widetilde{\mu}_j\}_j$. In other words, non-contributing wave modes whose wave parameters might exhibit magnitudes close to one are removed from the reduced basis, as opposed to the classic procedure. This explains why the present model reduction strategy yields reduced bases of relative small sizes. The relevance of this strategy for computing the forced response of waveguides is highlighted hereafter.

---

[7]i.e. the square of the magnitude of the total velocity, considering the three directions of space for solid finite elements and the transverse direction for plate elements.

Beam-like structure

A clamped beam-like structure with thick rectangular cross-section, whose left end is subjected to a uniform force field, is considered (cf. Figure 1(a)). The material and geometric characteristics of the structure are: Young's modulus $E = 2 \times 10^{11}$ Pa, density $\rho = 7800$ kg.m^{-3}, Poisson's ratio $\nu = 0.3$, loss factor $\eta = 0.01$, length $L = 2$ m and cross-section area $h_y \times h_z = 0.2$ m $\times$ 0.3 m. The waveguide is discretized by means of 200 identical substructures, each of these being discretized by means of 4×6 linear finite elements (see Figure 1(a)). In this case, the number of incident / reflected wave modes involved for computing the forced response of the waveguide is $n = 105$. Using a reduced wave basis $\{\widetilde{\boldsymbol{\Phi}}_j\}_j$ with say $m = 30$ incident / reflected wave modes selected by means of the classic procedure (see above) yields the forced response to be computed as shown in Figure 3(a), over a frequency band $\mathcal{B}_f = [10 \text{ Hz}, 10^4 \text{ Hz}]$. Compared to the reference FE solutions involving the full discretized waveguide, the WFE formulation based on the reduced basis $\{\widetilde{\boldsymbol{\Phi}}_j\}_j$ with $m = 30$ incident / reflected wave modes appears as suffering from a lack of convergence for predicting the structure anti-resonances above 7000 Hz.

On the other hand, using the MOR strategy proposed in Section 3.4 yields the error bound $\mathcal{E}_s$ to be drawn as shown in Figure 4. As previously stated, the issue is to identify a minimum value of $\mathcal{E}_s$ with m small enough, while considering the assumptions $||\widetilde{\mathbf{A}}^s|| \leq ||\mathbf{A}^s||$ and $||\widetilde{\mathbf{A}}^{\star s}|| \leq ||\mathbf{A}^{\star s}||$ as valid (cf. green shaded areas in Figure 4). The minimum value of $\mathcal{E}_s$ clearly appears when the number of incident / reflected modes is $m = 26$. Here, $\mathcal{E}_s$ is close to zero (say under 0.1%) which means that the WFE solution is likely to be highly accurate. The fact that such a clear minimum point can be sought follows from the consideration of the

relative errors $(\epsilon_1^{\mathbf{A}} + \epsilon_2^{\mathbf{A}})$ and $(\epsilon_1^{\mathbf{A}^\star} + \epsilon_2^{\mathbf{A}^\star})$ for deriving $\mathcal{E}_s$ (cf. Section 3.3.3). Considering $m = 26$ as the number of incident / reflected modes yields the forced response to be drawn as shown in Figure 5. As expected, the convergence of the WFE formulation is entirely satisfied over the whole frequency band.

Figure 4

Figure 5

Another way to test the accuracy of the MOR strategy proposed in this paper (cf. Section 3.4) is to compute the relative error $||\widetilde{\mathbf{q}}^{(k)} - \mathbf{q}^{(k)}||/||\mathbf{q}^{(k)}||$ involved for expressing the vector of displacements $\mathbf{q}^{(k)}$ over any substructure boundary k. Following the discussion at the end of Section 3.3.2, it can be stated that this relative error can be assessed by means of the minimum value of the error bound $\mathcal{E}_s$, which in the present case is small (under 0.1%). To check this feature, the relative error $||\widetilde{\mathbf{q}}^{(k)} - \mathbf{q}^{(k)}||/||\mathbf{q}^{(k)}||$ (as involved by the MOR strategy when 26 wave modes are selected (see above)) has been plotted as a function of the frequency, considering the left end of the structure (i.e. the substructure boundary $k = 1$, where the excitation sources are applied). The result is shown in Figure 6. Also, the relative error involved by the classic model reduction procedure with $m = 30$ incident / reflected wave modes has been plotted. As expected, the MOR strategy based on the consideration of the error bound $\mathcal{E}_s$ for selecting the wave modes appears accurate over the whole frequency band $\mathcal{B}_f$. It is shown that the relative error is of the same order as the minimum value of $\mathcal{E}_s$ over $\mathcal{B}_f$, say relatively small (it could be emphasized that the relative error exhibits a few peaks with high magnitudes localized at very low frequencies, which are meaningless: this is explained since the norm $||\mathbf{q}^{(1)}||$ can be very small at the structure anti-resonances, leading to high values of the relative error). In comparison, the relative error involved by the

43

classic procedure appears considerably high. It increases as the frequency does to reach 30% at 10^4 Hz. Again, this clearly proves the relevance of the MOR strategy proposed in the present paper.

Figure 6

Reissner-Mindlin plate

A square Reissner-Mindlin plate, with one edge subjected to a prescribed transverse displacement, is considered (cf. Figure 1(b)). The material and geometric characteristics of the structure are: Young's modulus $E = 2 \times 10^{11}$ Pa, density $\rho = 7800$ kg.m^{-3}, Poisson's ratio $\nu = 0.3$, loss factor $\eta = 0.01$, shear correction factor $\kappa = 5/6$, area $L_x \times L_y = 1$ m $\times$ 1 m, thickness $h = 0.002$ m. The waveguide (i.e. the plate) is discretized by means of 40 identical substructures along the $x-$direction. The FE model of a representative substructure is shown in Figure 1(b). It enables $n = 83$ incident / reflected wave modes to be computed for describing the forced response of the waveguide (see Section 2). Using the classic wave mode selection procedure requires the reduced wave basis to be considerably enlarged to reach the convergence of the WFE formulation [1]. For instance, using $m = 60$ incident / reflected wave modes yields the forced response of the waveguide to be computed as shown in Figure 3(b), over a frequency band $\mathcal{B}_f = [10 \text{ Hz}, 2000 \text{ Hz}]$. In this case, the WFE formulation suffers from a lack of convergence for predicting both structure resonances and anti-resonances, even at low frequency. The issue is that some contributing wave modes exhibit wave parameters $\{\widetilde{\mu}_j\}_j$ of very small magnitudes at low frequency (in other words, those wave modes are strongly evanescent). Such high order wave modes need to be

considered for capturing the highly fluctuating kinematic and mechanical fields, especially around the plate corners where prescribed displacements apply.

On the other hand, using the MOR strategy proposed in Section 3.4 yields the error bound $\mathcal{E}_s$ to be drawn as shown in Figure 7. As for the beam-like structure, a minimum value of $\mathcal{E}_s$ clearly appears (the predicted error is less than 1%). In this case, the sought number of incident / reflected wave modes is $m = 43$. Using these 43 modes in the WFE matrix formulation (cf. Eq. (15)) yields the forced response to be computed as shown in Figure 8. Again, the convergence of the method appears to be perfectly satisfied over the whole frequency band. In this case, the required number of wave modes appears considerably small compared to the classic selection procedure.

Figure 7

Figure 8

As it was the case with the beam-like structure, the relative error involved for expressing the vector of displacements over the left edge of the structure (substructure boundary 1) – i.e. $||\widetilde{\mathbf{q}}^{(1)} - \mathbf{q}^{(1)}||/||\mathbf{q}^{(1)}||$ – can be computed as a function of the frequency. The results provided by both MOR strategy based on the error bound $\mathcal{E}_s$ (i.e. with $m = 43$ incident / reflected wave modes) and classic procedure (i.e. with $m = 60$ incident / reflected wave modes) are shown in Figure 9. Again, the accuracy of the proposed MOR strategy is clearly highlighted; the relative error appears less than 1% over the whole frequency band. In other words, as stated in Section 3.3.2, the relative error is of the same order as the minimum value of $\mathcal{E}_s$ over $\mathcal{B}_f$.

Figure 9

Sandwich structure

A clamped three-layered structure, consisting of a soft rubber core surrounded by two stiff skins, is considered. The left end of the bottom skin is subjected to a uniform transverse force field (cf. Figure 1(c)). The material and geometric characteristics of the skins are: Young's modulus $E^s = 2.1 \times 10^{11}$ Pa, density $\rho^s = 7850$ kg.m^{-3}, Poisson's ratio $\nu^s = 0.3$, height $h^s = 2 \times 10^{-3}$ m and width 50×10^{-3} m. Also, the material and geometric characteristics of the core are: Young's modulus $E^c = 1.5 \times 10^6$ Pa, density $\rho^c = 950$ kg.m^{-3}, Poisson's ratio $\nu^c = 0.48$, height $h^c = 20 \times 10^{-3}$ m and width 50×10^{-3} m. The length of the sandwich structure is $L = 0.4$ m. Dissipation phenomena are accounted for by considering a same loss factor $\eta = 0.02$ for the three layers. The waveguide is discretized by means of 200 identical three-layered substructures, each of these being discretized using 4×1 linear elements for the skins and 4×4 linear elements for the core (see Figure 1(c)). The number of incident / reflected wave modes involved for computing the forced response of the waveguide is $n = 105$ (see Section 2). Using a reduced wave basis $\{\widetilde{\mathbf{\Phi}}_j\}_j$ with say $m = 80$ incident / reflected wave modes selected by means of the classic procedure (see above) yields the forced response as shown in Figure 3(c), over a frequency band $\mathcal{B}_f = [50\,\text{Hz}\,, 1500\,\text{Hz}]$. Compared to the reference FE solution when the full waveguide is discretized, the WFE formulation suffers from major drawbacks for predicting the structure resonances and anti-resonances above 1000 Hz, i.e. when the dynamics of the core are crucial.

Invoking the MOR strategy proposed in Section 3.4 yields the error bound $\mathcal{E}_s$ to be considered (cf. Figure 10). The result is not as obvious as for the previous cases (i.e. beam and plate). The error bound $\mathcal{E}_s$ appears as a monotonous decreas-

ing function of m (i.e. the number of retained wave modes) without clear minima. Regarding Eq. (62) and the discussions in Section 3.3.3, the issue is that the relative errors $(\epsilon_1^{\mathbf{E}} + \epsilon_2^{\mathbf{E}})$ and $(\epsilon_1^{\mathbf{E}^\star} + \epsilon_2^{\mathbf{E}^\star})$ exhibit values that are too large to balance the value of $(\epsilon_1^{\mathbf{A}} + \epsilon_2^{\mathbf{A}})$, $(\epsilon_1^{\mathbf{A}^\star} + \epsilon_2^{\mathbf{A}^\star})$. Such a problem does not seem unsolvable. Indeed, Figure 10 highlights two reasonable values of the error bound $\mathcal{E}_s$ for m small enough, i.e. $\mathcal{E}_s \approx 38\%$ when $m = 33$ and $\mathcal{E}_s \approx 18\%$ when $m = 63$. The respective WFE solutions are plotted in Figure 11. When $m = 33$, the WFE solution accuratly describes the structure behavior above 700 Hz but suffers from severe drawbacks at low frequencies. This is explained since the wave mode selection criterion is carried out at the highest frequency within $\mathcal{B}_f$ (see Section 3.4.2), i.e. some low-frequency contributing wave modes might have been neglected. Considering $m = 63$ incident / reflected wave modes with a lower error bound $\mathcal{E}_s$ clearly solves this issue. As expected, the required number of wave modes appears quite small compared to the classic selection procedure.

Figure 10

Figure 11

Again (see previous cases), the relative error $||\widetilde{\mathbf{q}}^{(1)} - \mathbf{q}^{(1)}||/||\mathbf{q}^{(1)}||$ can be computed as a function of the frequency, considering the vector of the displacements over the left boundary of the structure (substructure boundary 1) where the excitation sources are applied. The results provided by both MOR strategy – when 63 incident / reflected wave modes are selected by means of the error bound $\mathcal{E}_s$ – and classic procedure with 80 incident / reflected wave modes are shown in Figure 12. Again, the proposed MOR strategy appears more accurate compared to the classic procedure. Also, as stated in Section 3.3.2, the relative error provided by the proposed MOR strategy is of the same order as the value of $\mathcal{E}_s$ (say, below

47

18% when $m = 63$) over $\mathcal{B}_f$, except around $700 - 800$ Hz. The fact that the error bound is computed at the highest frequency considered within $\mathcal{B}_f$ (see Section 3.3.2) can explain in part this lack of accuracy, although the frequency response function depicted in Figure 11 is correctly predicted.

Figure 12

Two beam-like structures coupled with an elastic junction

Let us consider the coupled system depicted in Figure 1(d), involving two beam-like waveguides connected to an elastic junction (i.e. a quarter of torus). Apart from the coupling conditions, the other waveguide boundaries are respectively submitted to a uniform transverse force field and clamped end. The dynamic behavior of the coupled system has been investigated in a recent paper [18], over a frequency band $\mathcal{B}_f = [10\,\text{Hz}, 5000\,\text{Hz}]$ that enables the junction to undergo resonances. The two waveguides, as well as the coupling junction, exhibit the same material characteristics: Young's modulus $E = 3.2 \times 10^9$ Pa, density $\rho = 1180\,\text{kg.m}^{-3}$, Poisson's ratio $\nu = 0.39$, loss factor $\eta = 0.01$. The two waveguides have the same cross-sectional area $h_y \times h_z = 0.2\,\text{m} \times 0.15\,\text{m}$, while their respective lengths are $L_1 = 2\,\text{m}$ and $L_2 = 1.5\,\text{m}$. The quarter of torus has an internal radius of curvature of $R^{\text{c}} = 0.05$ m and a cross-section similar to those of the connected waveguides. The two waveguides exhibit the same cross-section and are discretized by means of similar substructures whose respective numbers are $N_1 = 100$ and $N_2 = 75$. Each substructure is meshed using 4×3 linear elements, yielding $n = 60$ incident / reflected wave modes to be considered for each waveguide for computing the forced response of the coupled system. A Lagrange

multipliers formalism that enables the junction and the waveguides to be meshed differently over the coupling interfaces is also considered [18]. Using two reduced wave basis $\{(\widetilde{\boldsymbol{\Phi}}_j)_1\}_j$ and $\{(\widetilde{\boldsymbol{\Phi}}_j)_2\}_j$ (for waveguides 1 and 2, respectively) e.g. consisting of $m_1 = m_2 = m = 30$ incident / reflected wave modes, selected by means of the classic procedure (see Section 5.1), yields the forced response of the coupled system to be described as shown in Figure 3(d). In this case, since the substructures used for both waveguides are similar, the reduced bases $\{(\widetilde{\boldsymbol{\Phi}}_j)_1\}_j$ and $\{(\widetilde{\boldsymbol{\Phi}}_j)_2\}_j$ turn out to be similar. It is shown that the WFE formulation suffers from a lack of convergence for predicting the system resonances and anti-resonances above 3000 Hz, i.e. when the local dynamics of the junction are of primary importance.

On the other hand, using the MOR strategy proposed in Section 4.3 yields the error bound $\mathcal{E}_s$ to be drawn as shown in Figure 13. In this case, since the wave modes are ranked independently for each waveguide (see Section 4.3), the reduced bases $\{(\widetilde{\boldsymbol{\Phi}}_j)_1\}_j$ and $\{(\widetilde{\boldsymbol{\Phi}}_j)_2\}_j$ turn out to be different. These are constituted individually considering the m most contributing incident / reflected wave modes for each waveguide. Considering Figure 13, a minimum value of $\mathcal{E}_s$ clearly appears, as expected (here, the predicted error is less than 0.001%!). The sought number of incident / reflected wave modes appears to be $m = 30$. Using such reduced bases $\{(\widetilde{\boldsymbol{\Phi}}_j)_1\}_j$ and $\{(\widetilde{\boldsymbol{\Phi}}_j)_2\}_j$ (i.e. constituted from the 30 most contributing incident / reflected wave modes for each waveguide) yields the forced response of the coupled system to be computed as shown in Figure 14. The convergence of the method completely agrees over the whole frequency band.

Figure 13

Figure 14

Again (see previous cases), the relative error $||\widetilde{\mathbf{q}}_1^{(1)} - \mathbf{q}_1^{(1)}||/||\mathbf{q}_1^{(1)}||$ can be

computed as a function of the frequency, considering e.g. the vector of the displacements over the left boundary of the waveguide 1 (substructure boundary 1) where the excitation sources are applied. The results are shown in Figure 15. Once more, the accuracy of the proposed MOR strategy is clearly highlighted compared to the classic procedure; considering the proposed MOR strategy yields the relative error to be less than 0.001% over the whole frequency band (as stated in Section 3.3.2, the relative error is correctly assessed by the minimum value of $\mathcal{E}_s$ over $\mathcal{B}_f$).

Figure 15

5.2. Application to a plate radiating in an acoustic fluid

The MOR strategy appears to be very efficient for saving large CPU time if for instance one considers the computation of the power radiated by a plate in a surrounding acoustic fluid. The fact that large CPU times are required for addressing this kind of problem is explained since coupling terms among wave modes (due to the fluid) occur, leading to the computation of a full square matrix of radiation impedance that is time consuming when many frequency steps are involved. In the present case, a square Reissner-Mindlin plate whose characteristics are similar to those depicted in Section 5.1 is considered. The structure is supposed to be surrounded by an infinite rigid baffle while radiating in an acoustic fluid (air) whose characteristics are: density $\rho_0 = 1 \text{ kg.m}^{-3}$ and celerity of waves $c_0 = 330 \text{ m.s}^{-1}$. The fluid is supposed to be inviscid and light, in the sense that its loading on the plate is neglected. For this kind of problem, a relevant approach is to compute the radiating power or, equivalently, the radiation efficiency. For this task, the method of elementary radiators can be used [19]. This suggests to "discretize" the plate

into elementary surfaces of same area $S_{radiator}$ and constant normal velocities, and to compute the radiation efficiency as

$$\sigma = \frac{\dot{\mathbf{q}}_n^H \mathbf{R} \dot{\mathbf{q}}_n}{\rho_0 c_0 S_{plate} < (\dot{\mathbf{q}}_n)^2 >}, \tag{83}$$

where $\dot{\mathbf{q}}_n$ is the vector of normal velocities of the elementary radiators, expressed as $\dot{\mathbf{q}}_n = \mathrm{i}\omega \mathbf{q}_n$ where $\mathbf{q}_n$ is the vector of normal displacements; also, $< (\dot{\mathbf{q}}_n)^2 >$ is the mean quadratic velocity averaged over all the elementary radiators, defined as

$$< (\dot{\mathbf{q}}_n)^2 > = \frac{1}{2} \frac{1}{N_{rad}} \sum_{k=1}^{N_{rad}} |(\dot{q}_n)_k|^2, \tag{84}$$

where N_{rad} is the total number of elementary radiators that are used for discretizing the plate, while $(\dot{q}_n)_k$ is the normal velocity of a given radiator k. Also, in Eq. (83), S_{plate} is the area of the plate while $\mathbf{R}$ is a full square matrix whose components are

$$R_{ij} = \frac{\omega^2 \rho_0 S_{radiator}^2}{4\pi c_0} \frac{\mathtt{sin}(k_0 r_{ij})}{k_0 r_{ij}} \quad (i \neq j) \quad , \quad R_{ii} = \frac{\omega^2 \rho_0 S_{radiator}^2}{4\pi c_0}, \tag{85}$$

where $k_0 = \omega/c_0$ is the acoustic wavenumber and r_{ij} is the distance between two radiators i and j. A typical elementary radiator is depicted in Figure 16, with an area $S_{radiator} = L_x/20 \times L_y/10$ ($L_x = 1$ m and $L_y = 1$ m being the length and width of the plate). The normal velocity of each radiator is supposed to be constant and equal to the normal velocity at its mid node (cf. Figure 16).

Figure 16

The WFE method can be used for approximating the vector of normal displacements (and thus the vector of normal velocities) of these radiators as $\mathbf{q}_n \approx \mathcal{L}' \widetilde{\boldsymbol{\Phi}}_{\mathbf{q}} \widetilde{\mathbf{Q}}$, where $\widetilde{\boldsymbol{\Phi}}_{\mathbf{q}} = [\widetilde{\boldsymbol{\Phi}}_{\mathbf{q}}^{\mathtt{inc}} \widetilde{\boldsymbol{\Phi}}_{\mathbf{q}}^{\mathtt{ref}}]$ ($\widetilde{\boldsymbol{\Phi}}$ being the matrix of wave modes $\{\widetilde{\boldsymbol{\Phi}}_j\}_j$), $\widetilde{\mathbf{Q}} = [\widetilde{\mathbf{Q}}^{\mathtt{inc}T} \widetilde{\mathbf{Q}}^{\mathtt{ref}T}]^T$ is the vector of wave amplitudes and $\mathcal{L}'$ is an incidence matrix for capturing the normal displacements at the relevant DOFs. Thus, the

numerator appearing on the right hand side of Eq. (83) can be written as

$$\dot{\mathbf{q}}_n^H \mathbf{R} \dot{\mathbf{q}}_n = \omega^2 \sum_{i \geq 1} \widetilde{\mathbf{Q}}^H \left[\boldsymbol{\mu}'^{(i-1)H} \widetilde{\boldsymbol{\Phi}}_{\mathsf{q}}^H \mathcal{L}'^H \mathbf{R}_{ii} \mathcal{L}' \widetilde{\boldsymbol{\Phi}}_{\mathsf{q}} \boldsymbol{\mu}'^{(i-1)} \right] \widetilde{\mathbf{Q}} \qquad (86)$$

$$+ 2\omega^2 \sum_{i \geq 1} \sum_{j > i} \mathtt{Re} \left\{ \widetilde{\mathbf{Q}}^H \left[\boldsymbol{\mu}'^{(i-1)H} \widetilde{\boldsymbol{\Phi}}_{\mathsf{q}}^H \mathcal{L}'^H \mathbf{R}_{ij} \mathcal{L}' \widetilde{\boldsymbol{\Phi}}_{\mathsf{q}} \boldsymbol{\mu}'^{(j-1)} \right] \widetilde{\mathbf{Q}} \right\},$$

where $\widetilde{\mathbf{Q}}$ is to be understood as the vector of wave amplitudes for the radiators located at the left end of the plate; also, $\boldsymbol{\mu}'$ is a diagonal matrix with components $\{\widetilde{\mu}_j^\alpha\}_j$ ($\{\widetilde{\mu}_j\}_j$ being the wave parameters already introduced in Section 2.1), where α is an integer that "scales" the length d of a plate substructure (see Figure 1(b)) to the length of a radiator (i.e. $L_x/20$): in the present case, $\alpha = 2$; finally, $\mathbf{R}_{ij}$ is a square matrix extracted from the matrix $\mathbf{R}$ (see above) and which relates the coupling between two rows of radiators i and j, distant from $|i - j|L_x/20$. Otherwise, expressing the denominator on the right hand side of Eq. (83) by means of WFE wave modes does not add any more difficulty.

Regarding Eq. (86), the feature of the WFE approach is that the matrix terms inside the square brackets do not depend on the plate boundary conditions. Once these terms have been computed, the computation of the radiation efficiency can be investigated for several kinds of boundary conditions with fewer CPU times compared to the FE method. Nonetheless, even in the WFE framework, the CPU times remain substantial. Indeed, the computation of the radiation efficiency based on Eq. (86) requires many matrix multiplications and summations (for instance, the second term in square brackets needs to be computed 190 times) that have to be considered at many discrete frequencies. To highlight this point, it is proposed to compute the radiation efficiency considering 1041 discrete frequencies uniformly spread on a frequency band $\mathcal{B}_f = [10\,\text{Hz}, 2000\,\text{Hz}]$ (cf. Figure 17). Considering the full wave basis (here, the number of incident / reflected modes is $n = 83$ (see Section 5.1)) yields the CPU time to be 11h 2min 12s using an Intel® Core™ 2

52

Duo processor. Thus, reducing the sizes of the matrices and vectors involved in Eq. (86) efficiently appears crucial for lowering this computational cost. Considering the reduced wave basis provided by the MOR strategy with 43 incident / reflected modes (as established in Section 5.1), instead of the full wave basis, yields the radiation efficiency to be computed as shown in Figure 17. The result appears to be perfectly similar to those obtained when the full wave basis is considered, as expected. But the main advantage of the MOR strategy lies in the fact that the CPU time has been considerably reduced to $1\mathrm{h}\,27\mathrm{min}\,24\mathrm{s}$. This yields the CPU time to be reduced of 87% compared to the case when the full wave basis is considered. From this point of view, the relevance of the proposed MOR strategy is clearly highlighted.

Figure 17

5.3. Application to coupled waveguides involving junctions with uncertain eigen-frequencies

Another way to highlight the relevance of the proposed MOR strategy for saving large CPU times is to consider Monte Carlo simulations (MCS) involving many iterations. Such an analysis has already been investigated in a former paper [18] considering two waveguides coupled with an elastic junction whose eigenfrequencies exhibit slight uncertainties, i.e. when each junction eigenfrequency $\widetilde{\omega}_j/2\pi$ is perturbed as $\widetilde{\omega}_j^0 + \delta\widetilde{\omega}_j$ with $|\delta\widetilde{\omega}_j/\widetilde{\omega}_j^0| \leq 5\%$. In the work [18], a total number of $m^{\mathsf{c}} = 19$ vibrational modes for the junction has been considered, while $m = 50$ incident / reflected wave modes have been used for each waveguide. The MOR strategy proposed in the present work suggests that this number of wave modes can be

53

reduced to $m = 30$ without penalizing the description of the waveguide behavior (see Section 5.1). The results of MCS with 100 arbitrary trials for the 19 junction eigenfrequencies are shown in Figure 18, considering respectively $m = 50$ wave modes (classic approach) and $m = 30$ wave modes (MOR strategy) for the waveguides. Also, the component-wise bounds of the frequency response function – as derived in ref. [18] – have been highlighted. The results provided by the MOR strategy appear similar to those provided by the classic wave mode selection procedure, as expected. The feature of the proposed MOR strategy is that it requires $38 \text{min} \, 25 \text{s}$ for performing those MCS against $1 \text{h} \, 9 \text{min} \, 38$ s when the conventional procedure is considered. This yields a reduction of the CPU time of 45%.

Figure 18

6. Concluding remarks

A MOR strategy has been proposed within the wave finite element (WFE) framework for selecting the wave modes which are relevant for computing the LF and MF forced response of elastic waveguides. Single and coupled finite waveguides under prescribed forces or displacements have been investigated. The proposed approach is based on the reduction of error norms for describing the displacements and forces along the waveguides. The strategy for expressing these error norms consists in considering a finite number of forward and backward passings of waves along the waveguides. The fact that a few wave passings are considered is the key idea behind the proposed MOR strategy. This enables the selection of the wave modes to be carried out in a qualitative way, i.e. considering the minimization

54

of an error bound which increases when the sizes of the wave bases are overestimated. In many cases, the selection strategy provides a clear and unique answer to the number of wave modes which are to be retained for any waveguide. The MOR strategy enables the sizes of the wave bases to be reduced significantly compared to the conventional approach, i.e. when the wave modes are selected with regard to the magnitudes of their eigenvalues. The accuracy of the MOR strategy has been clearly highlighted in both single and coupled waveguide cases. Also, its relevance in terms of CPU time savings has been highlighted considering the computation of the acoustic radiation of a square baffled plate, as well as Monte Carlo simulations of a coupled system involving a junction with uncertain eigenfrequencies.

Appendix A. Bound of $||\widetilde{\mathbf{Q}}^{\mathtt{inc}(k)} - \widetilde{\mathcal{L}}\mathbf{Q}^{\mathtt{inc}(k)}||$

Considering Eqs. (41) and (42), $\widetilde{\mathbf{Q}}^{\mathtt{inc}(k)} - \widetilde{\mathcal{L}}\mathbf{Q}^{\mathtt{inc}(k)}$ is written as

$$\widetilde{\mathbf{Q}}^{\mathtt{inc}(k)} - \widetilde{\mathcal{L}}\mathbf{Q}^{\mathtt{inc}(k)} = \widetilde{\mathbf{E}}_s^{(k)} - \widetilde{\mathcal{L}}\mathbf{E}_s^{(k)} + \sum_{q=1}^{\infty} \left(\widetilde{\mathbf{A}}_k^{sq}\widetilde{\mathbf{E}}_s^{(k)} - \widetilde{\mathcal{L}}\mathbf{A}_k^{sq}\mathbf{E}_s^{(k)} \right)$$
$$k = 1, \dots, N+1 \quad \forall s \geq s_0. \quad \text{(A-1)}$$

A bound of $||\widetilde{\mathbf{Q}}^{\mathtt{inc}(k)} - \widetilde{\mathcal{L}}\mathbf{Q}^{\mathtt{inc}(k)}||$ readily follows as

$$||\widetilde{\mathbf{Q}}^{\mathtt{inc}(k)} - \widetilde{\mathcal{L}}\mathbf{Q}^{\mathtt{inc}(k)}|| \leq ||\widetilde{\mathbf{E}}_s^{(k)} - \widetilde{\mathcal{L}}\mathbf{E}_s^{(k)}|| + \sum_{q=1}^{\infty} ||\widetilde{\mathbf{A}}_k^{sq}\widetilde{\mathbf{E}}_s^{(k)} - \widetilde{\mathcal{L}}\mathbf{A}_k^{sq}\mathbf{E}_s^{(k)}||$$
$$k = 1, \dots, N+1 \quad \forall s \geq s_0. \quad \text{(A-2)}$$

Further investigation of this bound follows from the consideration that $\widetilde{\mathbf{A}}_k^{sq}\widetilde{\mathbf{E}}_s^{(k)} = \widetilde{\mathbf{A}}_k^{sq}(\widetilde{\mathbf{E}}_s^{(k)} - \widetilde{\mathcal{L}}\mathbf{E}_s^{(k)}) + \widetilde{\mathbf{A}}_k^{sq}\widetilde{\mathcal{L}}\mathbf{E}_s^{(k)}$, which yields

$$\widetilde{\mathbf{A}}_k^{sq}\widetilde{\mathbf{E}}_s^{(k)} - \widetilde{\mathcal{L}}\mathbf{A}_k^{sq}\mathbf{E}_s^{(k)} = \widetilde{\mathbf{A}}_k^{sq}(\widetilde{\mathbf{E}}_s^{(k)} - \widetilde{\mathcal{L}}\mathbf{E}_s^{(k)}) + (\widetilde{\mathbf{A}}_k^{sq}\widetilde{\mathcal{L}} - \widetilde{\mathcal{L}}\mathbf{A}_k^{sq})\mathbf{E}_s^{(k)}$$
$$k = 1, \dots, N+1 \quad \forall s \geq s_0. \quad \text{(A-3)}$$

From the consistency property of the 2−norm (see Section 2.4.1), Eq. (A-3) leads to $||\widetilde{\mathbf{A}}_k^{sq}\widetilde{\mathbf{E}}_s^{(k)} - \widetilde{\mathcal{L}}\mathbf{A}_k^{sq}\mathbf{E}_s^{(k)}|| \leq ||\widetilde{\mathbf{A}}_k^s||^q||\widetilde{\mathbf{E}}_s^{(k)} - \widetilde{\mathcal{L}}\mathbf{E}_s^{(k)}|| + ||\widetilde{\mathbf{A}}_k^{sq}\widetilde{\mathcal{L}} - \widetilde{\mathcal{L}}\mathbf{A}_k^{sq}||\,||\mathbf{E}_s^{(k)}||$ (to derive this inequality, it has been considered that $||\widetilde{\mathbf{A}}_k^{sq}|| \leq ||\widetilde{\mathbf{A}}_k^s||^q$). As a result, Eq. (A-2) yields

$$
\begin{aligned}
&||\widetilde{\mathbf{Q}}^{\mathtt{inc}(k)} - \widetilde{\mathcal{L}}\mathbf{Q}^{\mathtt{inc}(k)}|| \\
&\leq \left(\sum_{q=0}^{\infty}||\widetilde{\mathbf{A}}_k^s||^q\right)||\widetilde{\mathbf{E}}_s^{(k)} - \widetilde{\mathcal{L}}\mathbf{E}_s^{(k)}|| + \left(\sum_{q=1}^{\infty}||\widetilde{\mathbf{A}}_k^{sq}\widetilde{\mathcal{L}} - \widetilde{\mathcal{L}}\mathbf{A}_k^{sq}||\right)||\mathbf{E}_s^{(k)}|| \\
&\hspace{5cm} k = 1,\ldots,N+1 \quad \forall s \geq s_0. \quad \text{(A-4)}
\end{aligned}
$$

Appendix B. Bound of $||\mathcal{L}_{\mathbf{r}}\mathbf{Q}^{\mathtt{inc}(\boldsymbol{k})}||$

According to Eq. (41), $||\mathcal{L}_{\mathbf{r}}\mathbf{Q}^{\mathtt{inc}(k)}||$ is bounded as

$$
||\mathcal{L}_{\mathbf{r}}\mathbf{Q}^{\mathtt{inc}(k)}|| \leq ||\mathcal{L}_{\mathbf{r}}\mathbf{E}_s^{(k)}|| + \sum_{q=1}^{\infty}||\mathcal{L}_{\mathbf{r}}\mathbf{A}_k^{sq}\mathbf{E}_s^{(k)}||
$$
$$
k = 1,\ldots,N+1 \quad \forall s \geq s_0. \quad \text{(B-1)}
$$

Considering that $\mathcal{L}_{\mathbf{r}}\mathbf{A}_k^{sq}\mathbf{E}_s^{(k)} = \mathcal{L}_{\mathbf{r}}\mathbf{A}_k^{sq}\mathcal{L}_{\mathbf{r}}^T\mathcal{L}_{\mathbf{r}}\mathbf{E}_s^{(k)} + \mathcal{L}_{\mathbf{r}}\mathbf{A}_k^{sq}\widetilde{\mathcal{L}}^T\widetilde{\mathcal{L}}\mathbf{E}_s^{(k)}$ (because $\mathcal{L}_{\mathbf{r}}^T\mathcal{L}_{\mathbf{r}} + \widetilde{\mathcal{L}}^T\widetilde{\mathcal{L}} = \mathbf{I}_n$ (see above Proposition 1)), it turns out (from the consistency property of the 2−norm) that $||\mathcal{L}_{\mathbf{r}}\mathbf{A}_k^{sq}\mathbf{E}_s^{(k)}|| \leq ||\mathcal{L}_{\mathbf{r}}\mathbf{A}_k^{sq}\mathcal{L}_{\mathbf{r}}^T||\,||\mathcal{L}_{\mathbf{r}}\mathbf{E}_s^{(k)}|| + ||\mathcal{L}_{\mathbf{r}}\mathbf{A}_k^{sq}\widetilde{\mathcal{L}}^T||\,||\widetilde{\mathcal{L}}\mathbf{E}_s^{(k)}||$. Considering Eq. (B-1) and using the fact that $||\mathcal{L}_{\mathbf{r}}\mathbf{A}_k^0\mathcal{L}_{\mathbf{r}}^T|| = ||\mathcal{L}_{\mathbf{r}}\mathcal{L}_{\mathbf{r}}^T|| = 1$ (since $\mathbf{A}_k^0 = \mathbf{I}_n$ while the matrix $\mathcal{L}_{\mathbf{r}}^T$ is real orthogonal, i.e. $\mathcal{L}_{\mathbf{r}}\mathcal{L}_{\mathbf{r}}^T = \mathbf{I}_n$) yields

$$
||\mathcal{L}_{\mathbf{r}}\mathbf{Q}^{\mathtt{inc}(k)}|| \leq \left(\sum_{q=0}^{\infty}||\mathcal{L}_{\mathbf{r}}\mathbf{A}_k^{sq}\mathcal{L}_{\mathbf{r}}^T||\right)||\mathcal{L}_{\mathbf{r}}\mathbf{E}_s^{(k)}|| + \left(\sum_{q=1}^{\infty}||\mathcal{L}_{\mathbf{r}}\mathbf{A}_k^{sq}\widetilde{\mathcal{L}}^T||\right)||\widetilde{\mathcal{L}}\mathbf{E}_s^{(k)}||
$$
$$
k = 1,\ldots,N+1 \quad \forall s \geq s_0. \quad \text{(B-2)}
$$

The matrices $\widetilde{\mathcal{L}}^T$ and $\mathcal{L}_{\mathbf{r}}^T$ are unitary, which means that $||\widetilde{\mathcal{L}}^T|| = ||\mathcal{L}_{\mathbf{r}}^T|| = 1$ but also that $||\widetilde{\mathcal{L}}|| = ||\mathcal{L}_{\mathbf{r}}|| = 1$ (this is proved since $||\widetilde{\mathcal{L}}|| = ||\widetilde{\mathcal{L}}^T \widetilde{\mathcal{L}}||^{1/2} = ||\widetilde{\mathcal{L}}||^{1/2}$ and $||\mathcal{L}_{\mathbf{r}}|| = ||\mathcal{L}_{\mathbf{r}}^T \mathcal{L}_{\mathbf{r}}||^{1/2} = ||\mathcal{L}_{\mathbf{r}}||^{1/2}$, since the $2-$norm is unitarily invariant). Thus, according to the consistency property of the $2-$norm (see Section 2.4.1), $||\mathcal{L}_{\mathbf{r}} \mathbf{A}_k^{sq} \mathcal{L}_{\mathbf{r}}^T|| \leq ||\mathcal{L}_{\mathbf{r}}|| \, ||\mathbf{A}_k^s||_2^q ||\mathcal{L}_{\mathbf{r}}^T|| \leq ||\mathbf{A}_k^s||_2^q$ and $||\widetilde{\mathcal{L}} \mathbf{E}_s^{(k)}|| \leq ||\widetilde{\mathcal{L}}|| \, ||\mathbf{E}_s^{(k)}|| \leq ||\mathbf{E}_s^{(k)}||$. Therefore, Eq. (B-2) leads to

$$||\mathcal{L}_{\mathbf{r}} \mathbf{Q}^{\mathrm{inc}(k)}|| \leq \left(\sum_{q=0}^{\infty} ||\mathbf{A}_k^s||^q \right) ||\mathcal{L}_{\mathbf{r}} \mathbf{E}_s^{(k)}|| + \left(\sum_{q=1}^{\infty} ||\mathcal{L}_{\mathbf{r}} \mathbf{A}_k^{sq} \widetilde{\mathcal{L}}^T|| \right) ||\mathbf{E}_s^{(k)}||$$

$$k = 1, \ldots, N+1 \quad \forall s \geq s_0. \quad \text{(B-3)}$$

References

[1] J.-M. Mencik, On the low- and mid-frequency forced response of elastic systems using wave finite elements with one-dimensional propagation, Computers and Structures 88 (11-12) (2010) 674–689.

[2] Y. Waki, B. Mace, M. Brennan, Numerical issues concerning the wave and finite element method for free and forced vibrations of waveguides, Journal of Sound and Vibration 327 (1-2) (2009) 92–108.

[3] D. Duhamel, B. R. Mace, M. J. Brennan, Finite element analysis of the vibrations of waveguides and periodic structures, Journal of Sound and Vibration 294 (2006) 205–220.

[4] R. R. Craig, M. C. C. Bampton, Coupling of substructures for dynamic analyses, AIAA Journal 6 (7) (1968) 1313–1319.

[5] A. C. Antoulas, D. C. Sorensen, Approximation of large-scale dynamical systems: An overview, Technical Report, Electrical and Computer Engineering, Rice University, Houston, TX, 2001.

[6] D. Givoli, P. E. Barbone, I. Patlashenko, Which are the important modes of a subsystem?, International Journal for Numerical Methods in Engineering 59 (2004) 1657–1678.

[7] P. E. Barbone, D. Givoli, I. Patlashenko, Optimal modal reduction of vibrating structures, International Journal for Numerical Methods in Engineering 57 (2003) 341–369.

[8] B.-S. Liao, Z. Bai, W. Gao, The important modes of subsystems: A moment-matching approach, International Journal for Numerical Methods in Engineering 70 (13) (2007) 1581–1597.

[9] Z. Bai, Krylov subspace techniques for reduced-order modeling of large-scale dynamical systems, Applied Numerical Mathematics 43 (2002) 9–44.

[10] S. Gugercin, An iterative SVD-Krylov based method for model reduction of large-scale dynamical systems, Linear Algebra and its Applications 428 (2008) 1964–1986.

[11] E. J. Grimme, Krylov Projection Methods for Model Reduction, Ph.D. Thesis, ECE Department, University of Illinois, Urbana-Champaign.

[12] J. Fehr, P. Eberhard, M. Lehner, Improving the reduction process in flexible multibody dynamics by the use of 2ND order position gramian matrices, Proceedings of ENOC, St Petersburg, Russia.

[13] D. J. Mead, A general theory of harmonic wave propagation in linear periodic systems with multiple coupling, Journal of Sound and Vibration 27 (2) (1973) 235–260.

[14] W. X. Zhong, F. W. Williams, On the direct solution of wave propagation for repetitive structures, Journal of Sound and Vibration 181 (3) (1995) 485–501.

[15] J.-M. Mencik, M. N. Ichchou, Multi-mode propagation and diffusion in structures through finite elements, European Journal of Mechanics - A/Solids 24 (5) (2005) 877–898.

[16] C. Wilcox, Theory of Bloch waves, Journal d'Analyse Mathématique 33.

[17] J.-M. Mencik, M. N. Ichchou, L. Jézéquel, Propagation multimodale dans les systèmes périodiques couplés (in French), Revue Européenne de Mécanique Numérique 15 (1-3) (2006) 293–306.

[18] J.-M. Mencik, Model reduction and perturbation analysis of wave finite element formulations for computing the forced response of coupled elastic systems involving junctions with uncertain eigenfrequencies, Computer Methods in Applied Mechanics and Engineering 200 (45-46) (2011) 3051–3065.

[19] S. J. Elliott, M. E. Johnson, Radiation modes and the active control of sound power, Journal of the Acoustical Society of America 94 (4) (1993) 2194–2204.

List of Figures

Figure 1: Illustration of several elastic waveguides and representative substructures: (a) beam-like structure; (b) plate; (c) sandwich structure; (d) coupled beam-like structures.

Figure 2: Representation of substructure boundaries (their number is $N + 1$ along the waveguide) and representation of the conventions made to describe the incident / reflected waves at the left and right boundaries of waveguides.
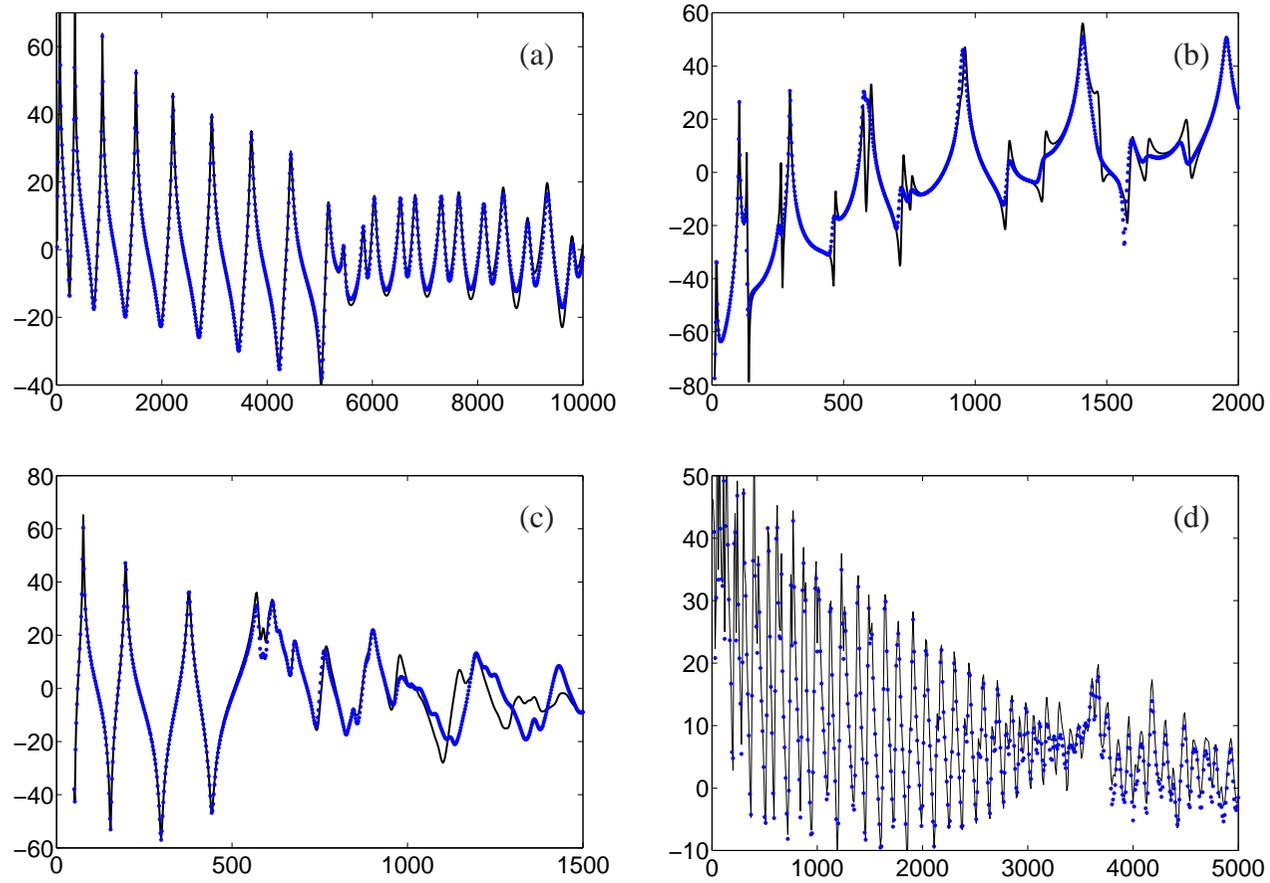
Figure 3: Frequency response function (quadratic velocity (dB)) for beam-like structure (a), plate (b), sandwich structure (c), coupled system (d): (———) FE reference solution; (● ● ●) WFE solutions when the wave modes are selected by the classic procedure (number of retained wave modes: $m = 30$ (a), $m = 60$ (b), $m = 80$ (c) and $m = 30$ (d)).
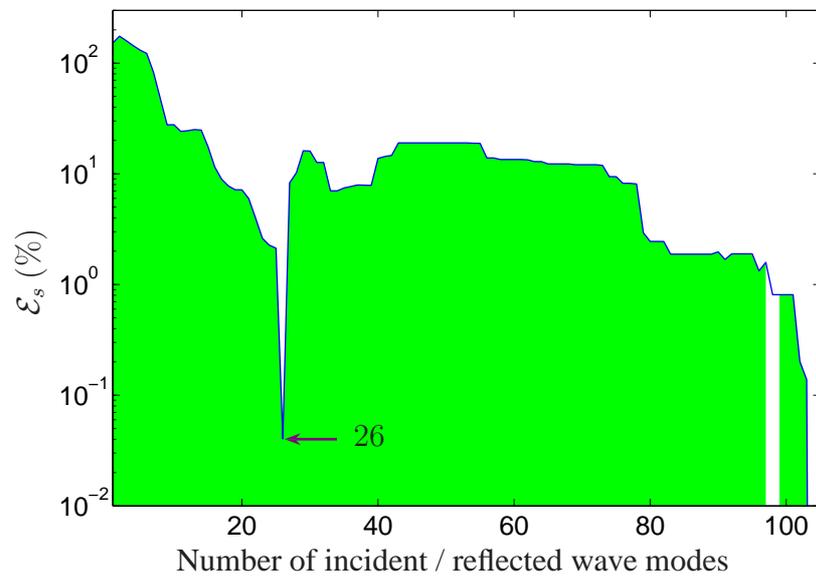
Figure 4: Error bound $\mathcal{E}_s$ as a function of the number m of incident / reflected wave modes for a clamped beam-like structure whose left end is subjected to a uniform transverse force field. (Green shaded area): case where assumptions $||\widetilde{\mathbf{A}}^s|| \leq ||\mathbf{A}^s||$ and $||\widetilde{\mathbf{A}}^{\star s}|| \leq ||\mathbf{A}^{\star s}||$ are satisfied.
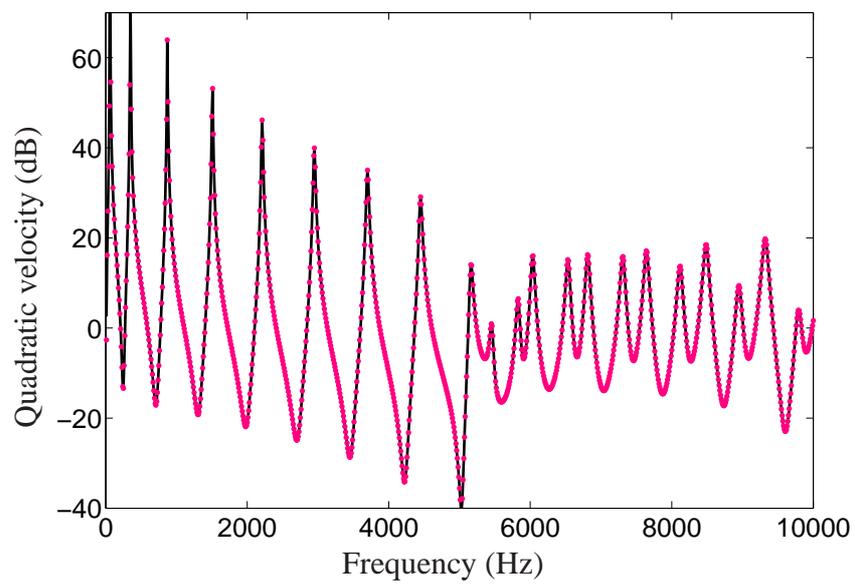
Figure 5: Frequency response function of a clamped beam-like structure whose left end is subjected to a uniform transverse force field: (———) FE reference solution; ($\bullet\,\bullet\,\bullet$) WFE solution with $m = 26$ wave modes selected by means of the error bound $\mathcal{E}_s$.
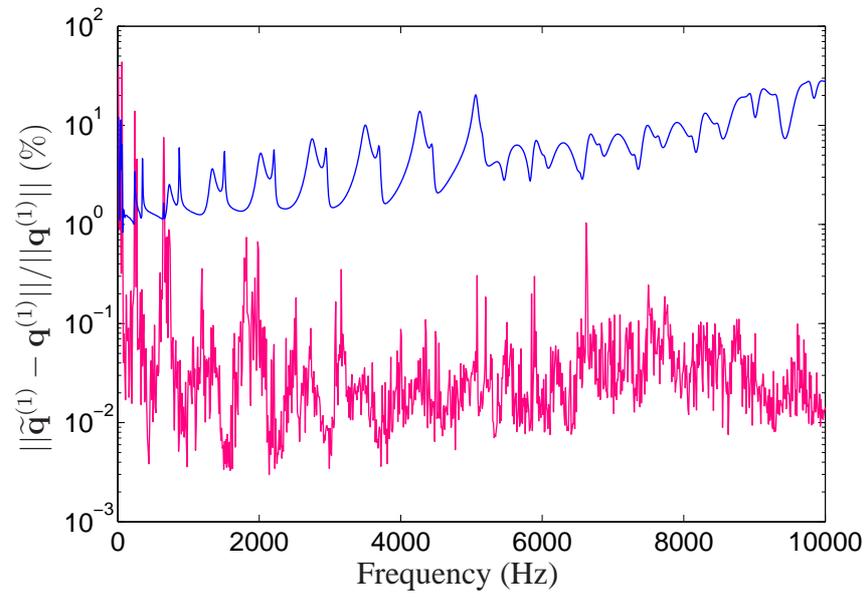
Figure 6: Relative error involved for expressing the vector of displacements over the left boundary of the beam-like structure: (———) WFE solution with $m = 30$ wave modes selected by means of the classic procedure; (———) WFE solution with $m = 26$ wave modes selected by means of the error bound $\mathcal{E}_s$.
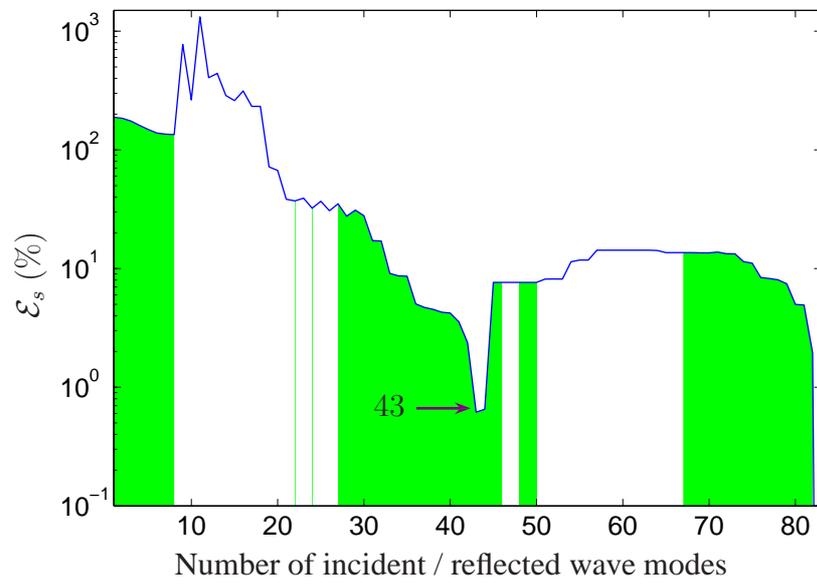
Figure 7: Error bound $\mathcal{E}_s$ as a function of the number m of incident / reflected wave modes for a Reissner-Mindlin plate with one edge subjected to a prescribed transverse displacement. (Green shaded area): case where assumptions $||\widetilde{\mathbf{A}}^s|| \leq ||\mathbf{A}^s||$ and $||\widetilde{\mathbf{A}}^{\star s}|| \leq ||\mathbf{A}^{\star s}||$ are satisfied.
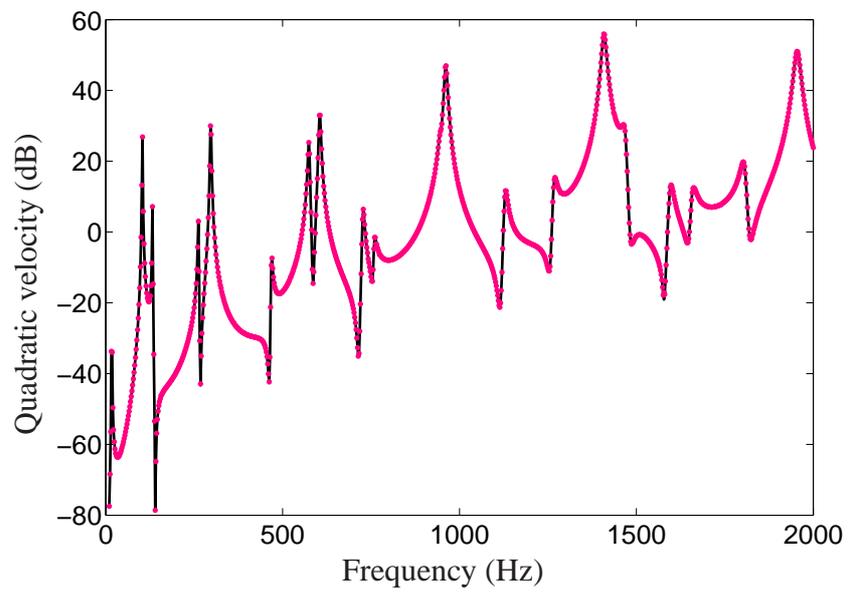
Figure 8: Frequency response function of a Reissner-Mindlin plate with one edge subjected to a prescribed displacement: (——) FE reference solution; (● ● ●) WFE solution with $m = 43$ wave modes selected by means of the error bound $\mathcal{E}_s$.
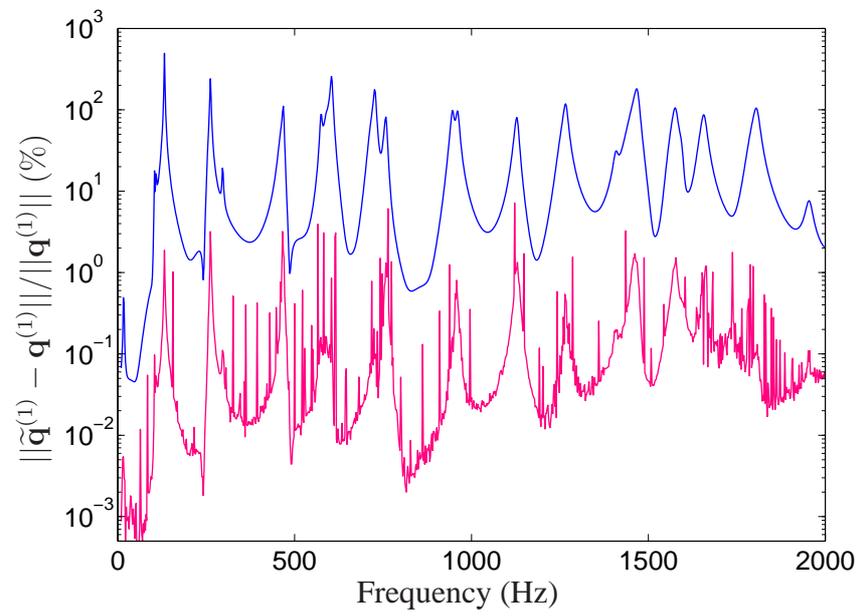
Figure 9: Relative error involved for expressing the vector of displacements over the left boundary of the plate: (———) WFE solution with $m = 60$ wave modes selected by means of the classic procedure; (———) WFE solution with $m = 43$ wave modes selected by means of the error bound $\mathcal{E}_s$.
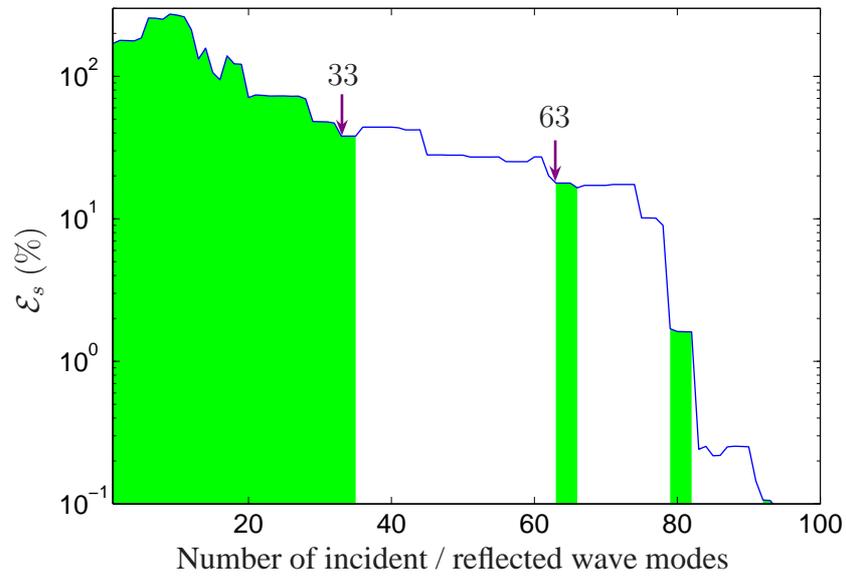
Figure 10: Error bound $\mathcal{E}_s$ as a function of the number m of incident / reflected wave modes for a clamped sandwich structure whose left boundary (bottom skin only) is subjected to a uniform transverse force field. (Green shaded area): case where assumptions $||\widetilde{\mathbf{A}}^s|| \leq ||\mathbf{A}^s||$ and $||\widetilde{\mathbf{A}}^{\star s}|| \leq ||\mathbf{A}^{\star s}||$ are satisfied.
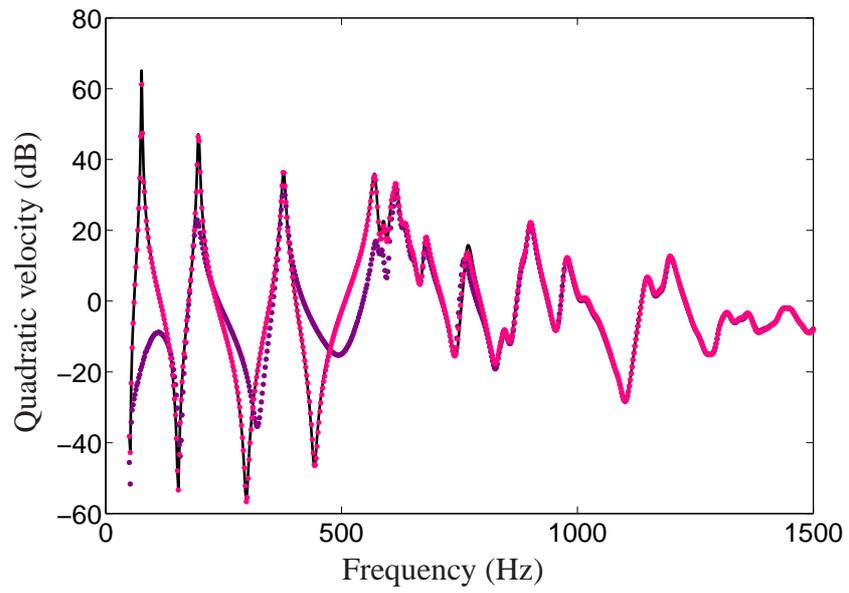
Figure 11: Frequency response function of a clamped sandwich structure whose left boundary (bottom skin only) is subjected to a uniform transverse force field: (——) FE reference solution; (● ● ●) WFE solution with $m = 33$ wave modes selected by means of the error bound $\mathcal{E}_s$; (● ● ●) WFE solution with $m = 63$ wave modes selected by means of the error bound $\mathcal{E}_s$.
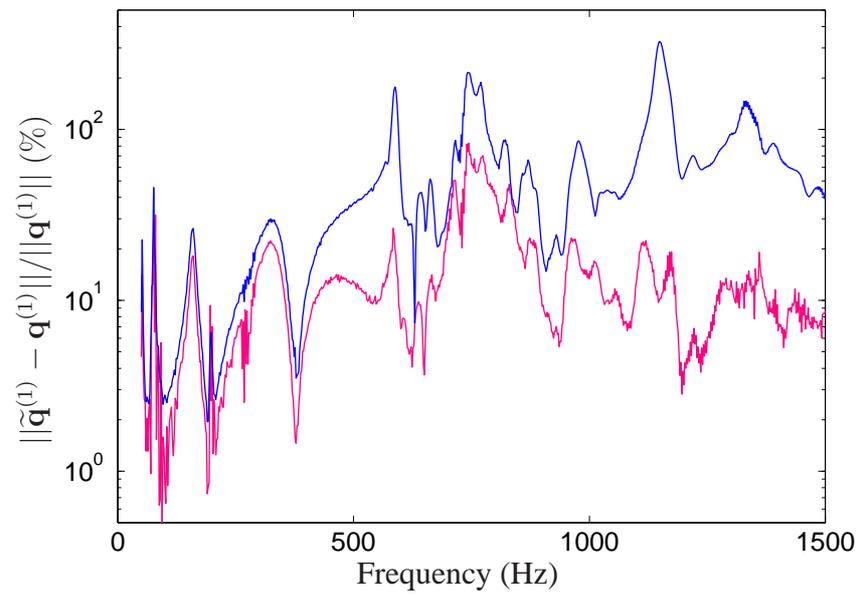
Figure 12: Relative error involved for expressing the vector of displacements over the left boundary of the sandwich structure: (———) WFE solution with $m = 80$ wave modes selected by means of the classic procedure; (———) WFE solution with $m = 63$ wave modes selected by means of the error bound $\mathcal{E}_s$.
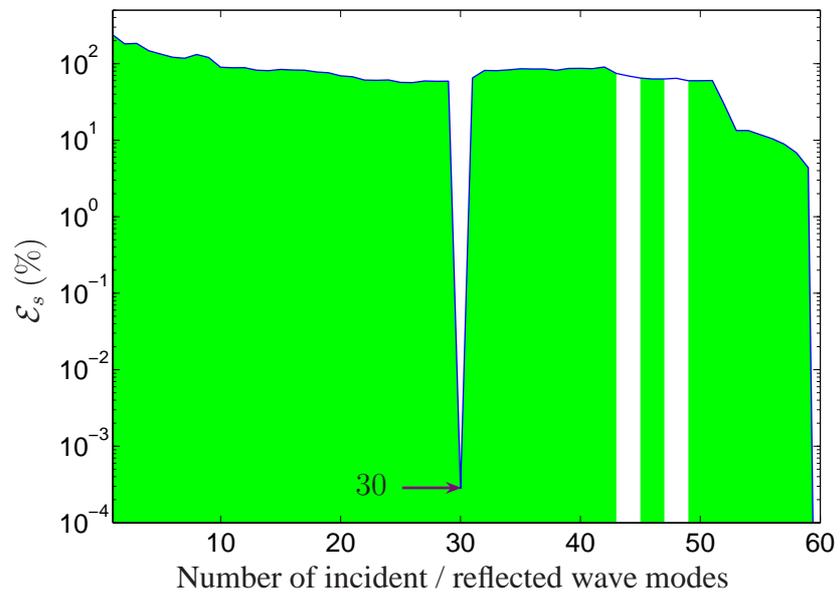
Figure 13: Error bound $\mathcal{E}_s$ as a function of the number m of incident / reflected wave modes for two coupled waveguides subjected to prescribed forces. (Green shaded area): case where assumptions $||\widetilde{\mathbf{A}}^s|| \leq ||\mathbf{A}^s||$ and $||\widetilde{\mathbf{A}}^{\star s}|| \leq ||\mathbf{A}^{\star s}||$ are satisfied.
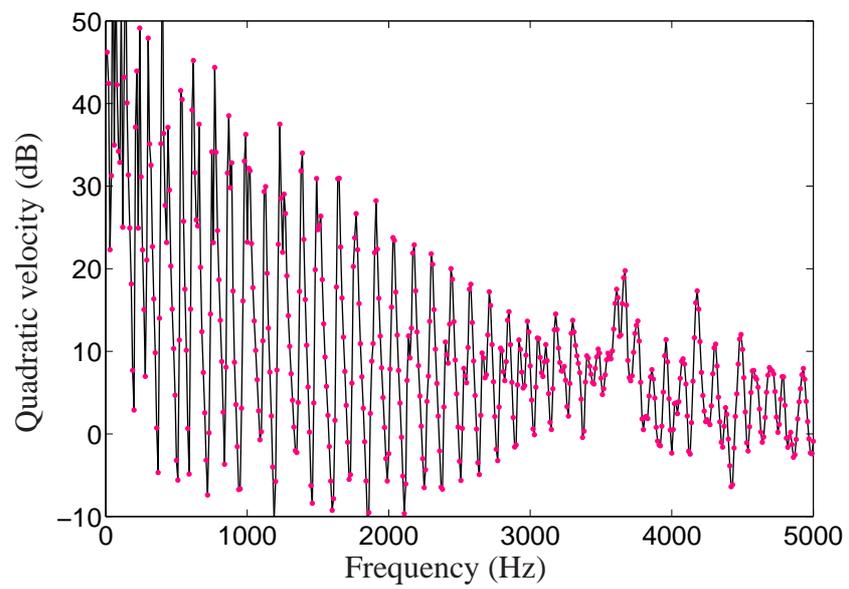
Figure 14: Frequency response function of two coupled waveguides subjected to prescribed forces: (——) FE reference solution; (● ● ●) WFE solution with $m = 30$ wave modes selected by means of the error bound $\mathcal{E}_s$.
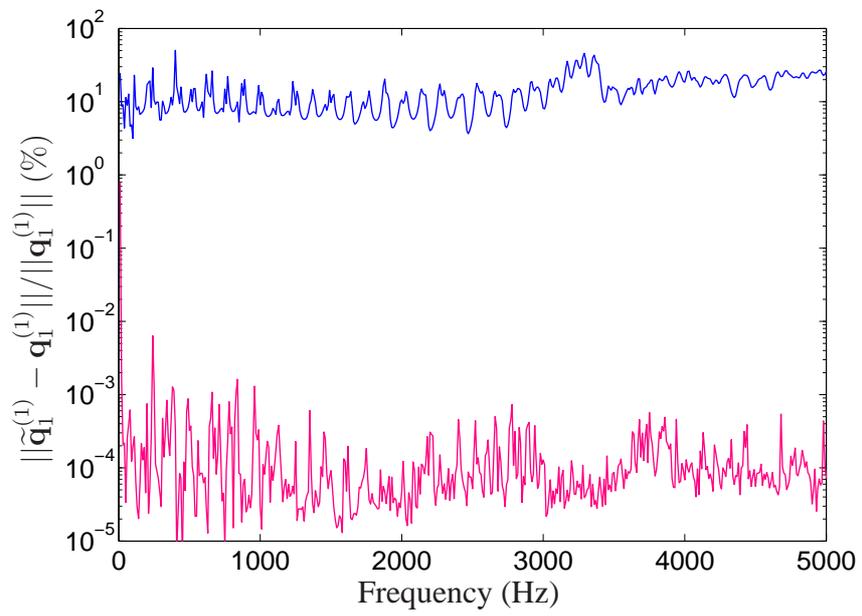
Figure 15: Relative error involved for expressing the vector of displacements over the left boundary of waveguide 1: (——) WFE solution with $m = 30$ wave modes selected by means of the classic procedure; (——) WFE solution with $m = 30$ wave modes selected by means of the error bound $\mathcal{E}_s$.
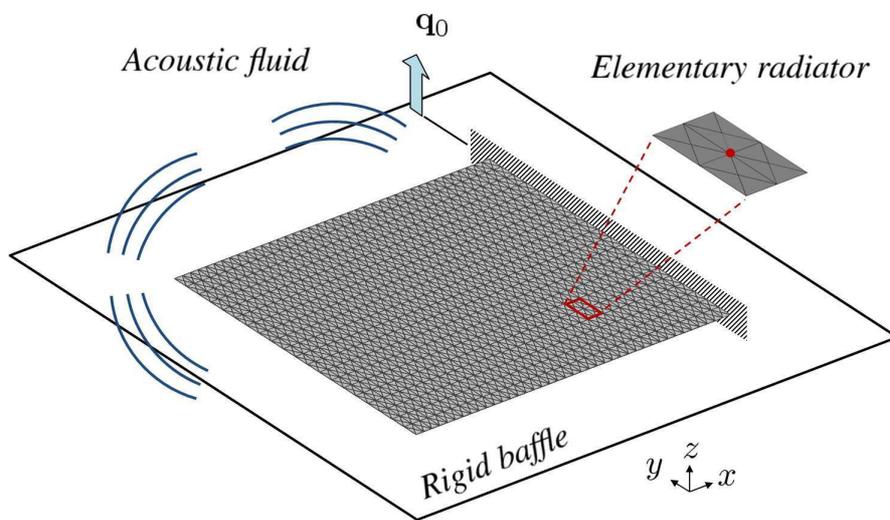
Figure 16: Illustration of a Reissner-Mindlin plate surrounded by a rigid baffle and radiating in a light acoustic fluid.
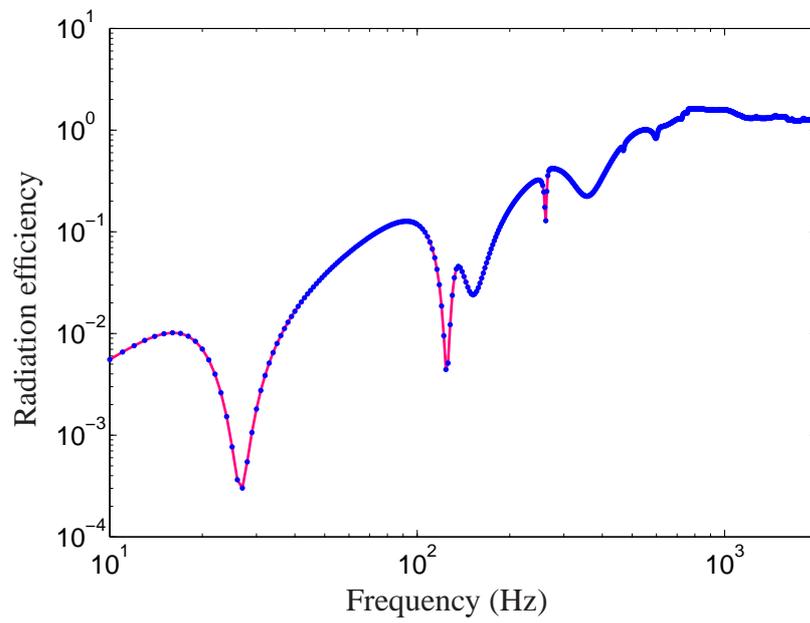
Figure 17: Radiation efficiency of a baffled Reissner-Mindlin plate, with one edge subjected to a prescribed transverse displacement, radiating in air: (● ● ●) WFE solution with the full wave basis; (——) WFE solution with the reduced wave basis provided by the MOR strategy.
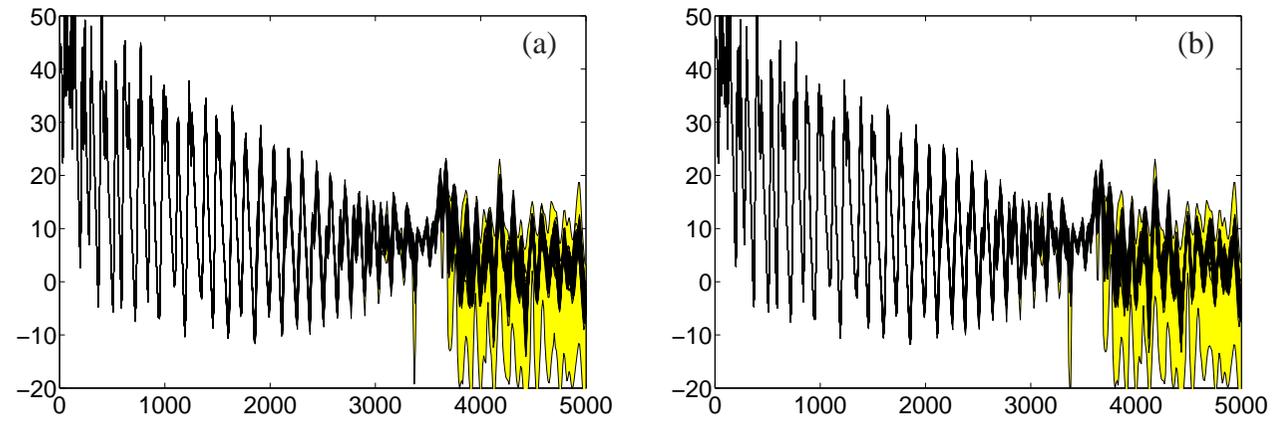
Figure 18: Frequency response function (quadratic velocity (dB)) of two waveguides connected to an elastic junction, using MCS (——) with 100 trials for the junction eigenfrequencies; (yellow shaded area) component-wise perturbation bounds: (a) solutions provided by the classic strategy using $m = 50$ wave modes; (b) solutions provided by the MOR strategy using $m = 30$ wave modes.